JOINT INSTITUTE FOR NUCLEAR RESEARCH

FRANK LABORATORY OF NEUTRON PHYSICS

Scientific Research Infrastructure of the FLNP: For Conducting Applied and Fundamental Research

Bagdaulet Mukhametuly

Frank Laboratory of Neutron Physics
at Joint Institute for Nuclear Research in Dubna

International School on Nuclear Methods and Applied Research in Environmental, Material and Life Sciences (NUMAR-GOBI-2025)
Ulaanbaatar, Mongolia: June 30 – July 4, 2025

Joint Institute for Nuclear Research

an international intergovernmental organization

Member States

Armenia, Cuba, Kazakhstan, Slovakia,
Azerbaijan, DPRK, Mongolia, Uzbekistan,
Belarus, Egypt, Romania, Vietnam,
Bulgaria, Georgia, Russia

Associate Members

Germany
Hungary
Italy
The Republic of South Africa
Serbia

Joint Coordinating Committee

Expert Working Group

JINR comprises 7 Laboratories, each being comparable with a large institute in the scale and scope of investigations performed

+ university center

900+ partner research organizations and universities from **60+** countries

Frank Laboratory of Neutron Physics


DLNP


BLTP


FLNR


FLNP


MLIT


LRB


VBLHEP


UNC

FLNP staff breakdown:

Total	557
Scientists	202
Engineers and specialists	152
Workers	171
Administrative staff	32

Average age – 48.1 years
Women – 27 %
Doctors – 29 persons
PhD – 108 persons
Foreigners – 96 persons

THREE MAIN SCIENTIFIC DEPARTMENTS of FLNP:

- **Department of nuclear physics** (139 persons)
- **Department of Neutron Investigations of Condensed Matter** (99 persons)
- **Department of Spectrometers Complex IBR-2** (51 persons)
- **+ Raman spectroscopy sector** (10 persons)
- **Sector of a new source and complex of moderators** (26 persons)

Neutrons:
Historical Background, Main Properties.

Discovery of the neutron

1919
Artificial splitting of nuclei by α-particles, hypothesis of a massive nucleus
Neutron as a combination of a proton and an electron.

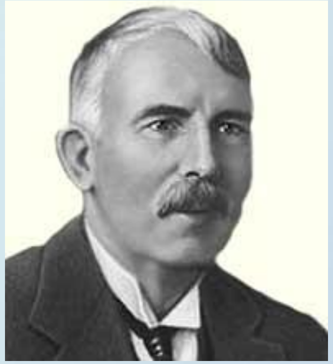

Ernest Rutherford
30.08.1871, NZ
19.10.1937, UK

1932
Discovery by J. Chadwick in experiments on irradiation of beryllium with alpha particles of penetrating radiation of particles with a mass close to the mass of a proton and zero charge.

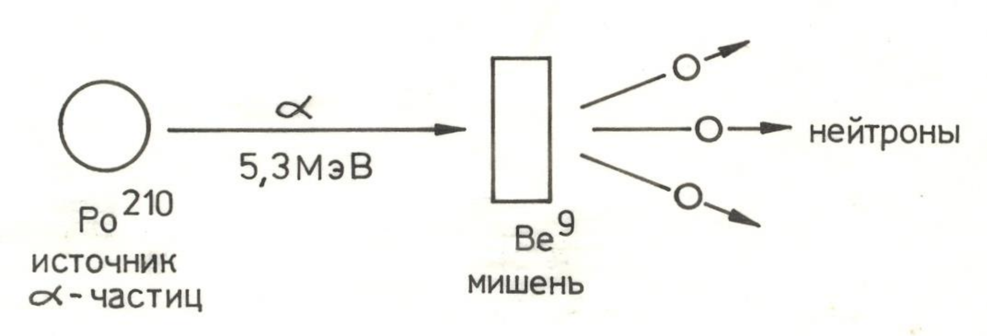

$$Be^9 + He^4 \rightarrow C^{12} + n + 5{,}7\ МэВ$$

James Chadwick
20.10.1891, UK
24.07.1974, UK

Properties of the Neutron

Year 1934
Slowing down of neutrons by hydrogen-containing substances (H2O, paraffin) to thermal energies.
On average, a fast neutron collides 19 times in water before slowing down.

Year 1938
Fission of uranium under the action of thermal neutrons.

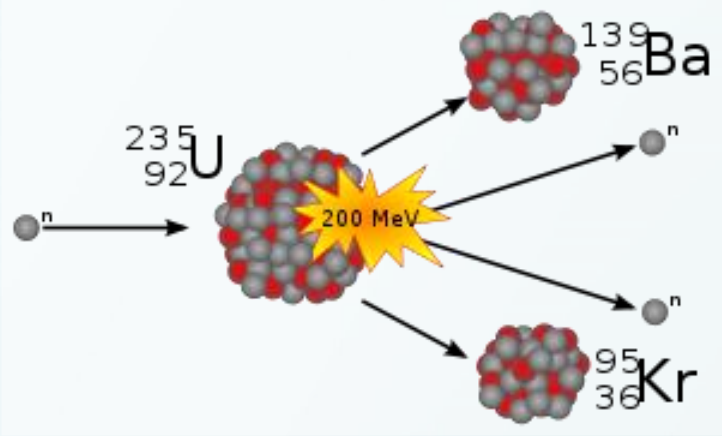

Enrico Fermi
29.09.1901, Italy
28.11.1954, USA

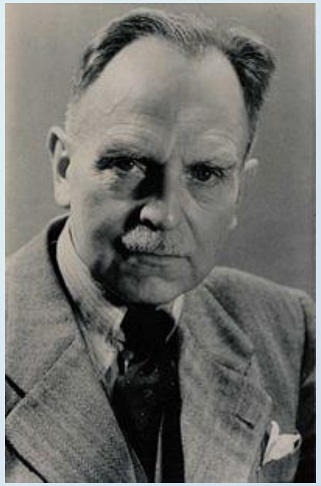

Otto Hahn;
1879 – 1968

Fritz Straßmann;
1902 -1980

The first nuclear reactor in ANL (Chicago)

Enrico Fermi

29.09.1901, Italy
28.11.1954, USA

Year 1942
“The Chicago Pile” – a drawing depicting the launch of the first nuclear reactor. Graphite blocks, between which are spheres of natural uranium. The chain reaction occurs on ^{235}**U,** the nuclei of which are split by thermal neutrons.

Development of Neutronography in the USSR

1946 – the first reactor in the USSR (Kurchatov Institute, Moscow)

On this wasteland in 1943, the future "Kurchatov Institute" was built.

In this building in 1946, the first chain reaction in Europe/Asia was carried out.

I.V. Kurchatov
30.12.1902, USSR
07.02.1960, USSR

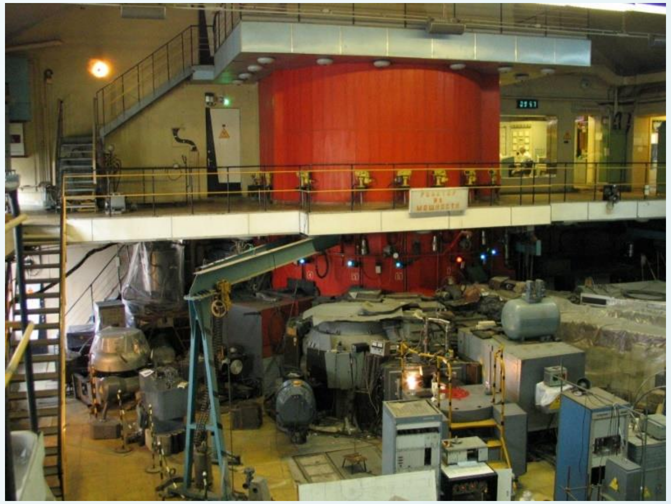

1957 – IRT – the first research reactor in the USSR

Neutron scattering

Neutron scattering - is a set of experimental methods for studying the structure and dynamic properties of condensed media at the atomic or molecular level using low-energy neutron scattering (thermal neutrons with a characteristic energy of ~ 0.02 eV, a wavelength of ~ 2 Å)

Main sections:

- structural neutron scattering (atomic structure)
- magnetic neutron scattering (magnetic structure)
- neutron spectroscopy (atomic and magnetic dynamics)

Main techniques:

- diffraction,
- small-angle scattering
- reflectometry,
- inelastic scattering.

Structural Neutron scattering

Determination using a neutron diffraction experiment of the main characteristics of the atomic structure of the crystal, which include:

- spatial symmetry
- parameters of the elementary cell
- coordinates of atoms
- thermal parameters of atoms
- position filling factors

Determination of the characteristics of the microstructure of the crystal, which include:

- size of crystallites (coherent blocks)
- macro and micro stresses
- crystallographic texture
- phase composition

Magnetic Neutron scattering

Determination using a neutron diffraction experiment of the main characteristics of the magnetic structure of the crystal, which include:

- parameters of the magnetic elementary cell
- wave vector of the magnetic structure
- coordinates of the magnetic atoms
- magnitude of the magnetic moments
- direction of the magnetic moments

Neutron spectroscopy

Determination using inelastic scattering of neutrons of the main characteristics of the dynamic movements of atoms or magnetic moments of the substance, which include:

- phonon spectrum of the crystal
- requencies of local oscillations
- dispersion curves
- diffusion movements
- effects of the electric field

Basic techniques in neutron scattering

Neutron diffraction on crystals – structure analysis with a resolution of 0.01 Å.

Neutron diffraction on amorphous solids – analysis of radial distribution with a resolution at the level of 1 Å.

Small-angle neutron scattering (SANS) - is an analysis of the geometric characteristics of large (10 – 1000 Å) inhomogeneities.

Neutron reflectometry - is an analysis of the distribution of scattering density along the normal to the interface between media, external or internal.

Polarized neutron scattering - is the analysis of the distribution of spin density or magnetization in a medium.

Neutron scattering in Dubna

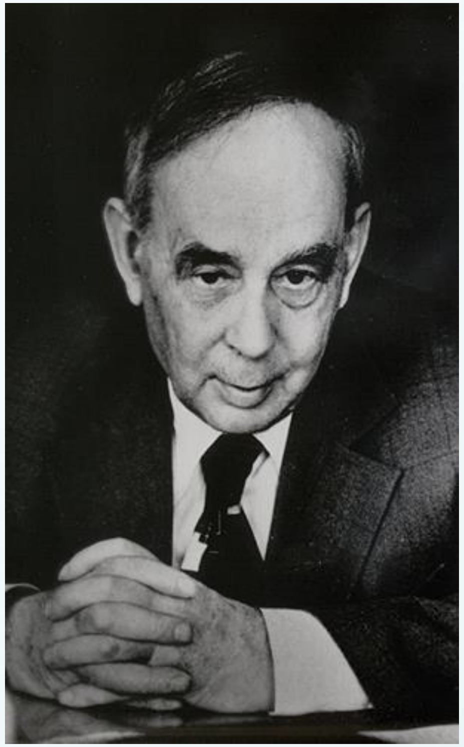

Ilya Mikhailovich Frank
1908 - 1990 

Dmitry Ivanovich Blokhintsev
1908 - 1979

- 1955 – Dimitry I. Blokhintsev (first director of JINR) - the idea of pulsed reactor
- 1960-1968-2001 – Ilya M. Frank & Fyodor L. Shapiro – the pulsed reactor IBR, IBR-30
- 1984-2010-204x – IBR-2, IBR-2M

Fedor Lvovich Shapiro
1915 - 1973

Pulsed reactors at the JINR Laboratory of Neutron Physics

1961 – 1968	IBR-1 (1 – 6 kW)
1969 – 1980	IBR-30 (15 kW)
1981 – 1983	IBR-2 (100 – 1000 kW)
1984 – 2006	IBR-2 (1500 – 2000 kW)
2007 – 2010	IBR-2 conversion
2011 – 204x	IBR-2M (2000 kW)

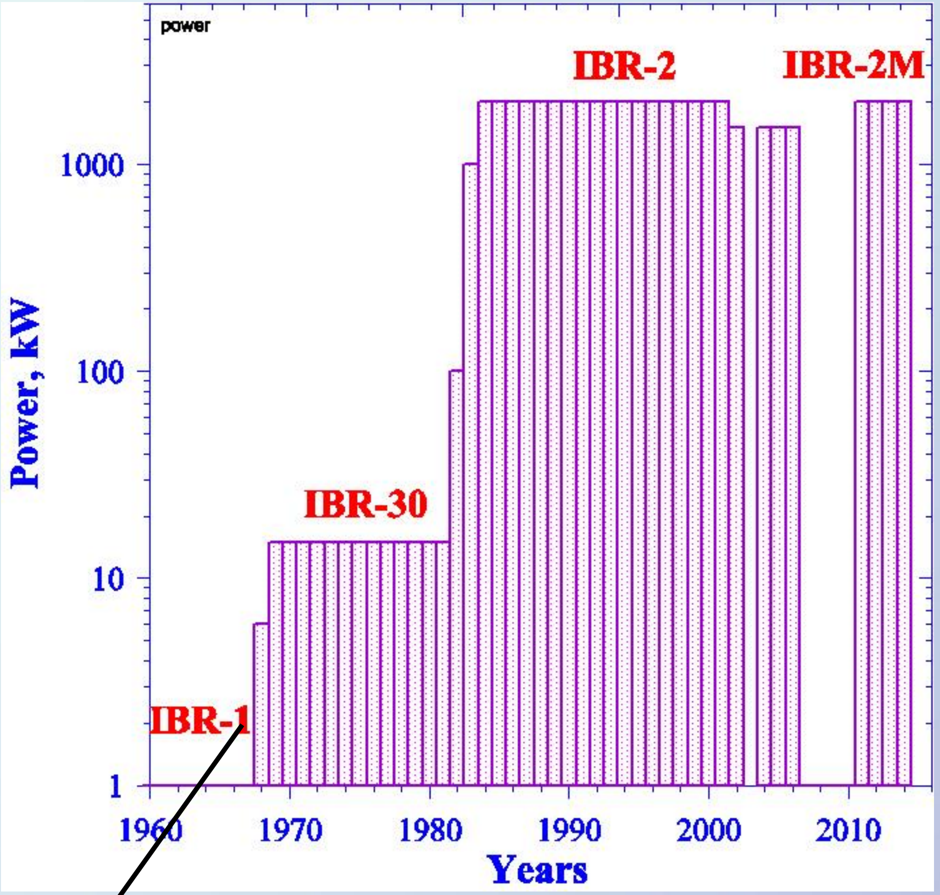

W = 1 kW
Commissioned in June 1960.

The building of the IBR-2 reactor

Experimental hall at the IBR-2 reactor

IBR-2 Pulsed Reactor

https://flnp.jinr.int/en-us/main/facilities/ibr-2

Operating since 1984

Deep modernization was carried out in 2006-2010

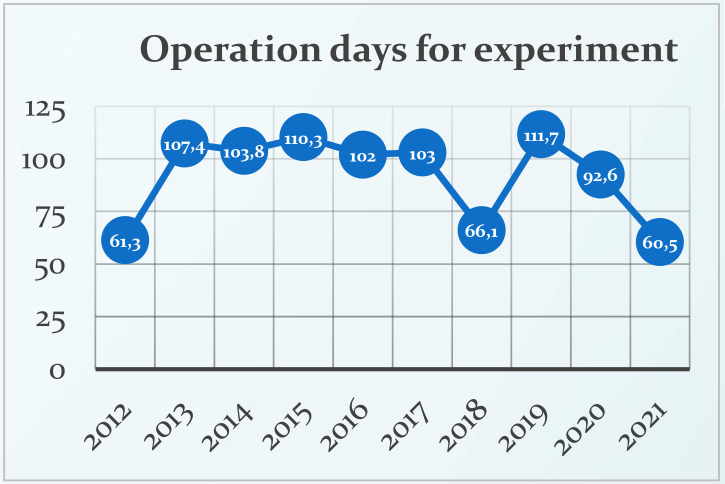

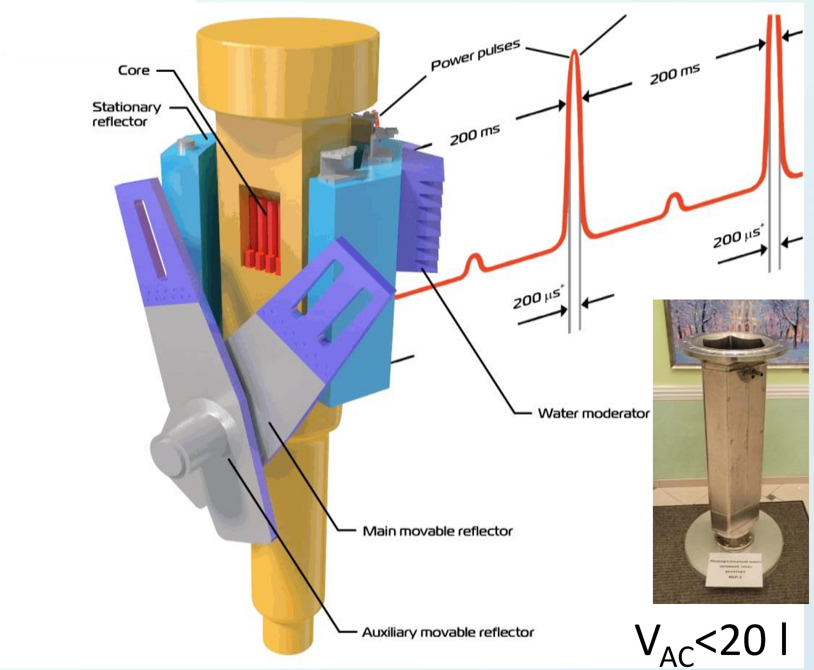

V_{AC}<20 l

- October 16, 2021 - February 17, 2025 – reactor **shutdown**
- **Resumption** of operation was done **in March 2025**

Average power, MW	**2**
Fuel	PuO_2
Pulse repetition rate, Hz	**5**
Pulse half-width, µs: fast neutrons thermal neutrons	 200* **340**
Rotation rate, rev/min • Main reflector • Auxiliary reflector	 600 300
Background, %	**7.5**
Thermal neutron flux density from the surface of the moderator • Time average • Burst maximum	 **~10^{13} n/cm² s** **~10^{16} n/cm² s**

* at reactor power of 2MW

prepared by Dr. D. Chudoba

Neutron Instruments

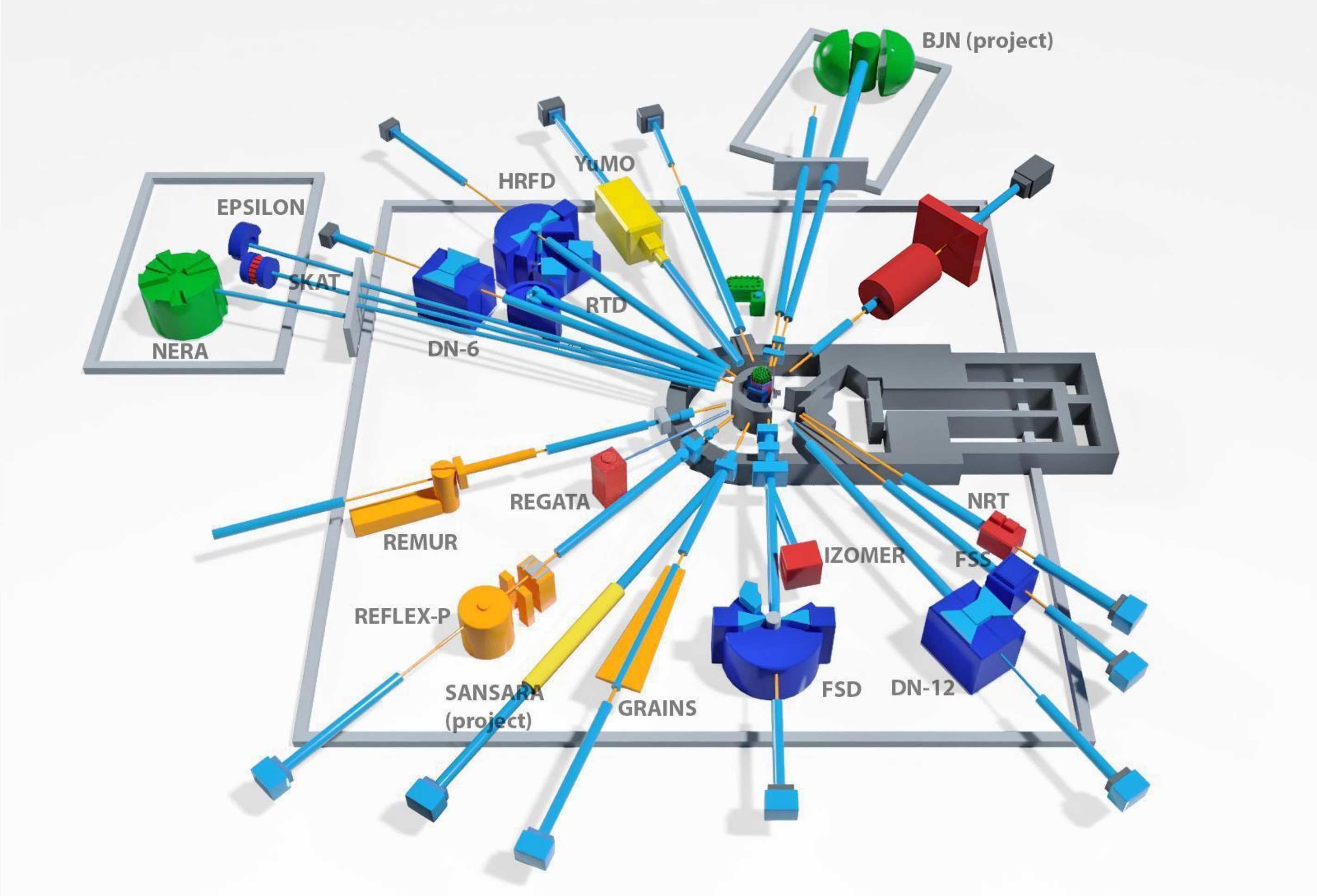

- Length of neutron guides – up to ~30 m in the experimental halls and up to ~100 m in two pavilions.
- Typical neutron flux density on the sample – ~10^6 cm^{-2}s^1 (up to 4 x 10^7 cm^{-2}s^1)

14 INSTRUMENTS INCLUDED IN USER PROGRAM

Diffraction:
HRFD
RTD
DN-6
EPSILON
SKAT
DN-12
FSD

Inelastic scattering:
NERA

Small-Angle
YuMo

Reflectometry:
GRAINS
REMUR
REFLEX

NAA:
REGATA

Under construction:
- **SANSARA** – small angle + imaging (2026)
- **BJN** – inelastic scattering (2027)

Parameters of the instruments could be found at https://flnp.jinr.int/en-us/main/facilities/ibr-2

NRT (neutron imaging) is included in the User Program in the second half of 2025

FLNP User Program

Who can apply for beam time?

- Scientists from **any country of the world** can apply for beam time.
- Scientists from member states of JINR get additional financial support.

https://ibr-2.jinr.int

I. Regular access applications

	First round	Second round
Period for proposal submission	September 1 - October 15	March 1 – April 15
Experiments time	1 half-year	2 half-year

https://flnp.jinr.int/en-us/main/your-experiment-at-flnp

Distribution of the beam time

In the FLNP JINR the neutron beam time at the high flux pulsed IBR-2 reactor is distributed between **internal users** (FLNP) and **general science community** (GSC) in the ratio of

- **35%** (internal proposals)
- **55%** (external regular proposals)
- **10%** (external urgent beam time requests)

II. Fast access applications

- NO DEADLINE
- Submission – via FLNP scientific secretary

FLNP User Program

The proposals are evaluated by **Experts Committees** (**technical and scientific**) and beam time for experiments is granted upon possibility of technical implementation and scientific merit of the proposal.

Scientific Experts Committees:

- Nanosystems and Soft Matter (YuMO, GRAINS, REFLEX, REMUR)
- Atomic and Magnetic Structure

  (RTD, DN-6, DN-12, SKAT, EPSILON, FSD, HRFD)
- Lattice and Molecular Dynamics (NERA)
- Neutron Activation Analysis (REGATA)

Detailed information could be found at:

Sidorov N.E., Chudoba D.M., Gorshkova Yu.E., Kochnev P.O., Sadovsky D.A. "User program for the neutron source reactor IBR-2 (FLNP JINR)" Physics of Particles and Nuclei Letters, ISSN 1547-4771, 2024, Vol. 21, No. 3, pp. 553–559.

JOINT INSTITUTE FOR NUCLEAR RESEARCH

FRANK LABORATORY OF NEUTRON PHYSICS

The priority research directions at the IBR-2 instruments:

1. Condensed Matter Physics and Materials Science;

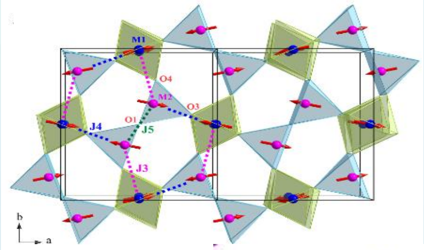

2. Physics of Nanosystems and Nanoscale Phenomena;

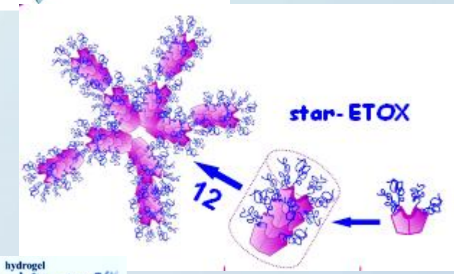

3. Physics of Complex Liquids and Polymers;

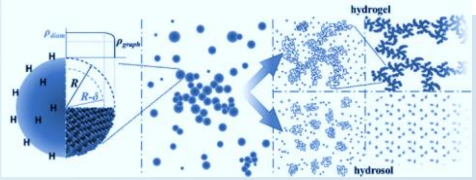

4. Biophysics and Pharmacology;

5. Applied Materials and Engineering Sciences.

Neutron scattering in condensed matter physics

Diffraction

Experimental facilities

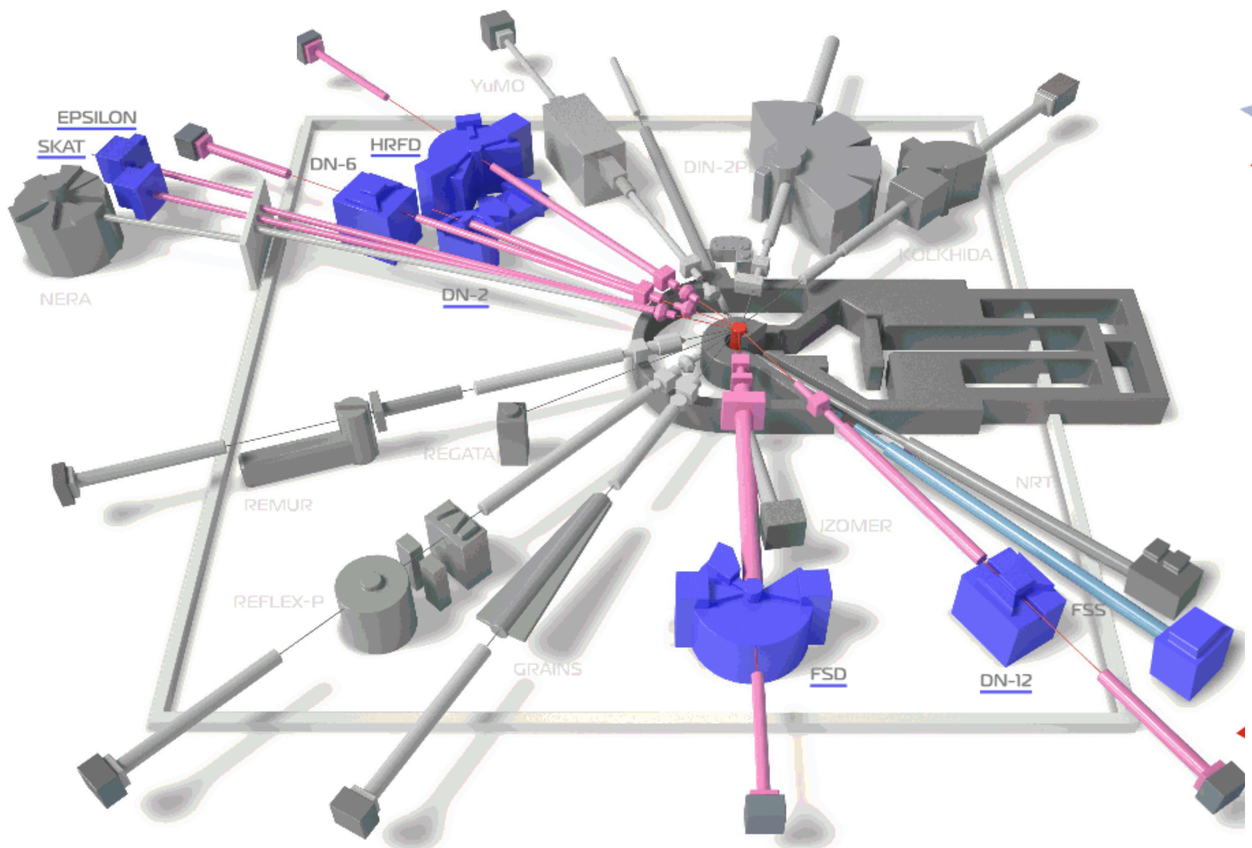

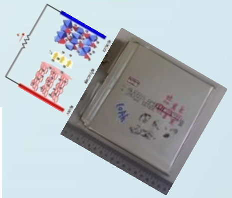

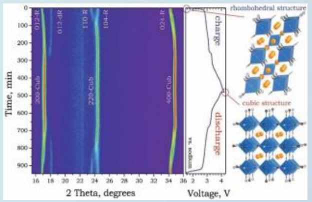

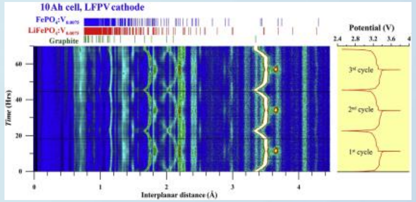

- Crystal and magnetic structure of novel materials under ambient and extreme conditions
- Real-time studies of Li-based accumulators
- Phase transitions of H-based storage alloys
- Crystallographic texture of metals, rocks and biological objects
- Strain measurements in structural materials
- 2D van der Waals magnetic materials

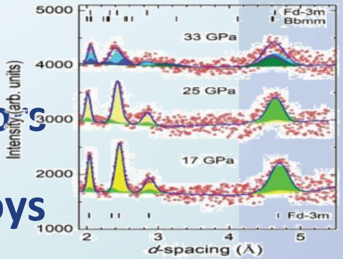

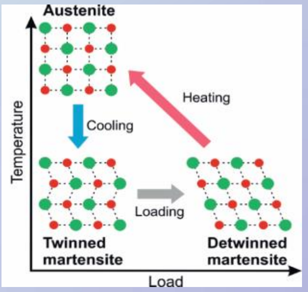

Diffractometers equipped with Fourier choppers to achieve high resolution at short beamlines with long pulse of the reactor

Scientific highlights

JOINT INSTITUTE FOR NUCLEAR RESEARCH

FRANK LABORATORY OF NEUTRON PHYSICS

High-Pressure Effects on Structural and Magnetic Properties of van der Waals Antiferromagnet $MnPS_3$

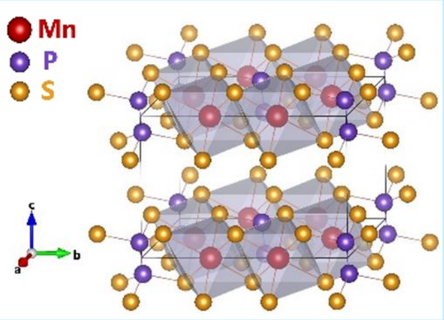

Monoclinic crystal structure of $MnPS_3$

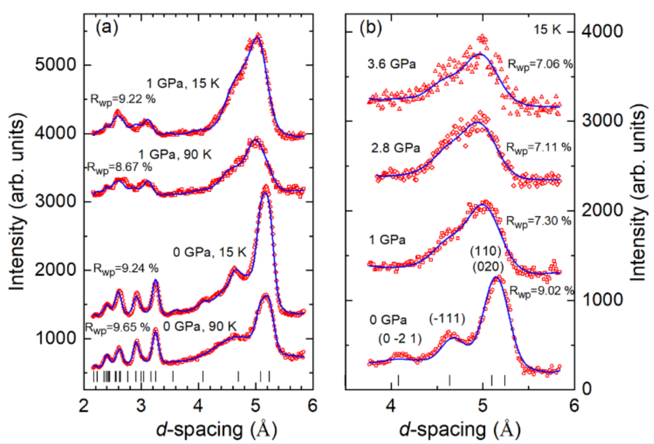

Neutron diffraction patterns of $MnPS_3$ at high pressures and selected temperatures

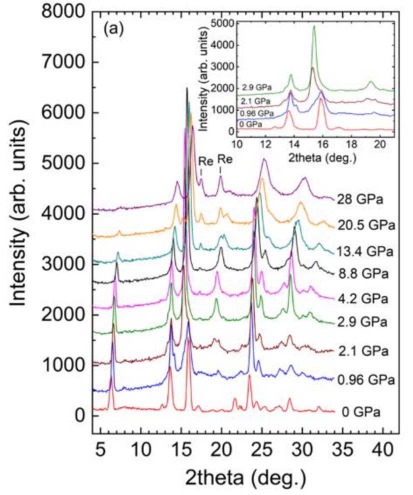

X-ray diffraction patterns of $MnPS_3$ at high pressures

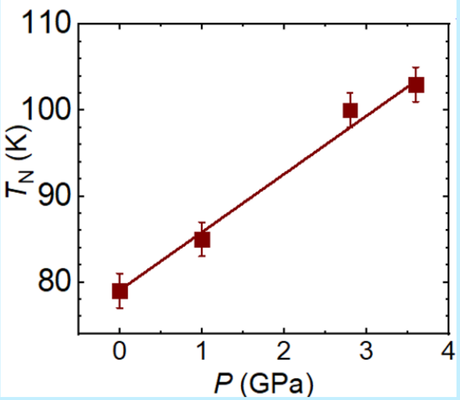

Pressure behavior of the Neel Temperature

D.P. Kozlenko, O.N. Lis, N.T.Dang et.al, Phys. Rev. Materials 8, 024402 (2024)

Pressure-Induced Ferroelectric – Paraelectric Phase Transition in $R_2Ti_2O_7$ (R=La, Pr, Nd)

The layered titanates demonstrate one of the highest known ferroelectric Curie temperatures (T_C > 1400 °C) and piezoelectric behavior with high coercive field (Eg > 45 kV/cm)

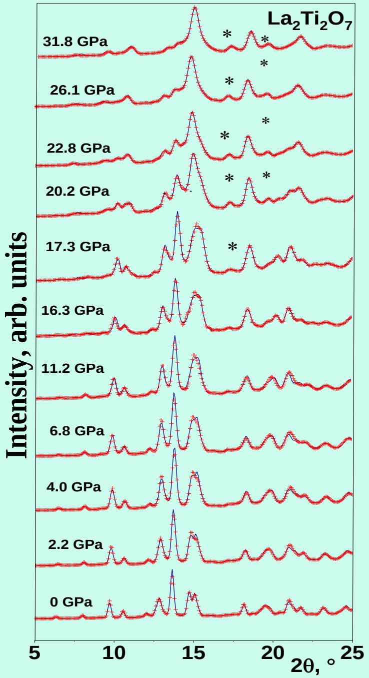

X-ray diffraction patterns of $La_2Ti_2O_7$ at high pressures

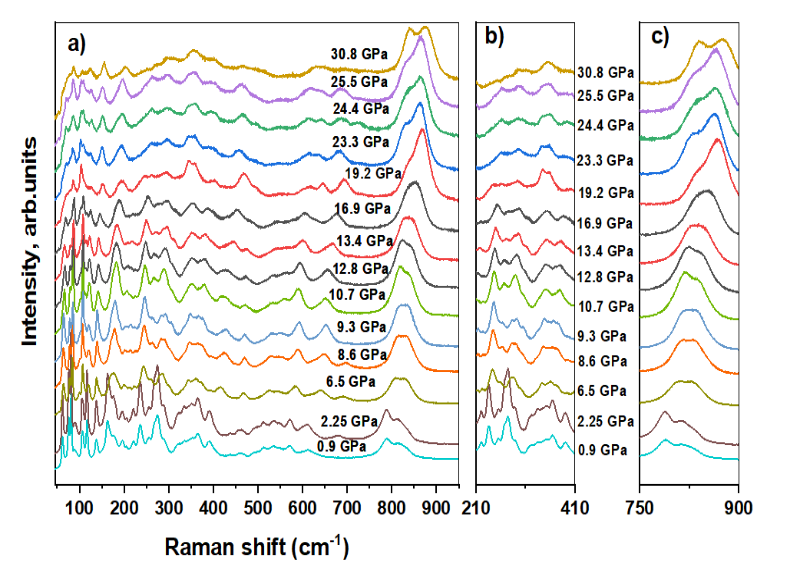

Raman spectra of $La_2Ti_2O_7$ at high pressures

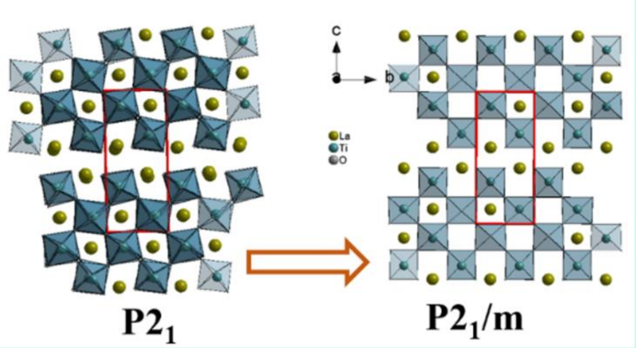

Structural re-arrangement caused by the ferroelectric – paraelectric phase transition in $R_2Ti_2O_7$ at high pressures

A.G.Asadov, D.P. Kozlenko, S.E. Kichanov, E.V.Lukin et.al, Journal of Alloys and Compounds 1003, 175461 (2024), Solid State Sciences 156, 107676 (2024)

Studies of the phase composition features of Fe-Ga alloys with increased gallium content

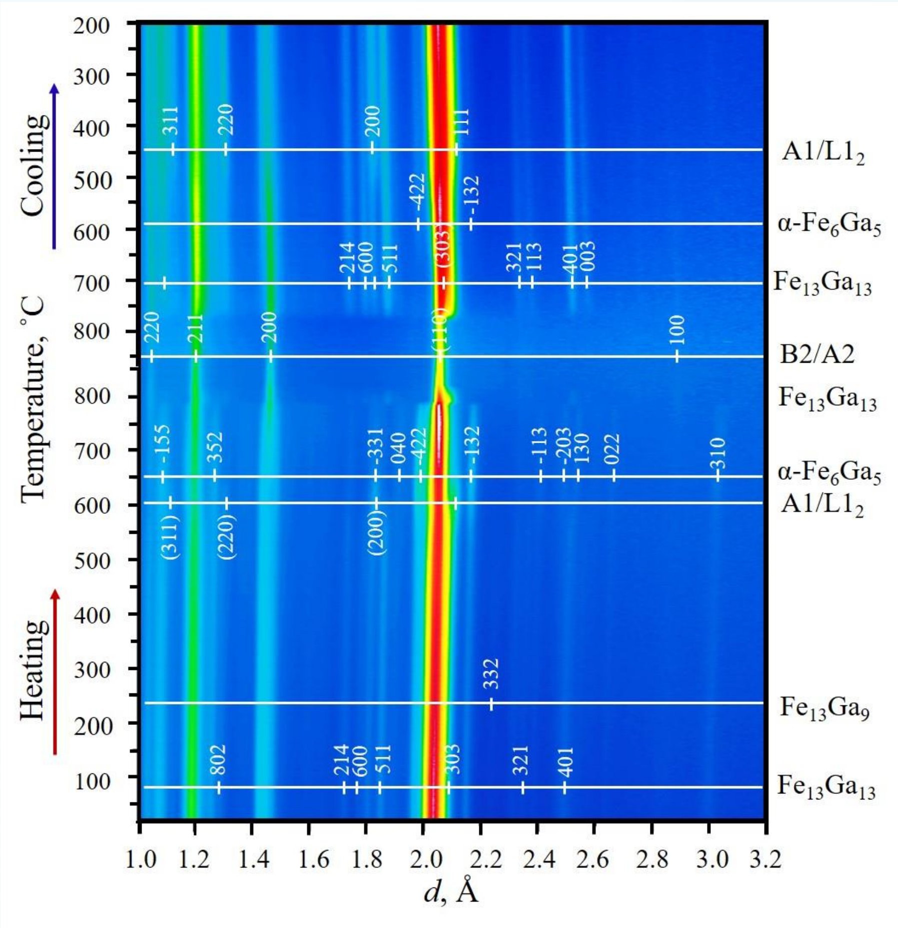

2D visualization of the evolution of diffraction patterns during heating and subsequent cooling of Fe-42Ga alloy.

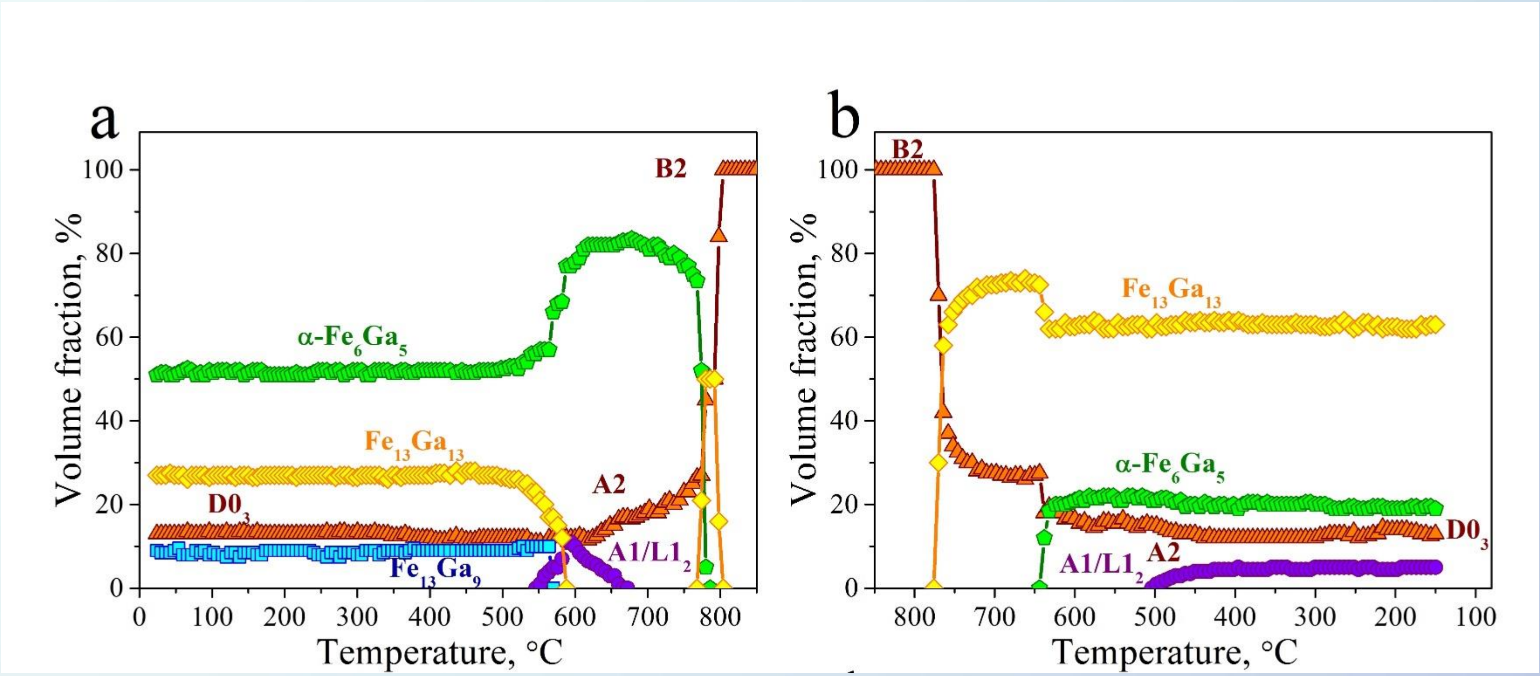

Evolution of the phase composition of the metastable Fe-42Ga alloy upon heating to 850° C (a) and cooling (b)

T. Vershinina et al., Journal of Alloys and Compounds, 1002, 175306 (2024)

Investigation of the Prussian white cathode material for sodium ion batteries

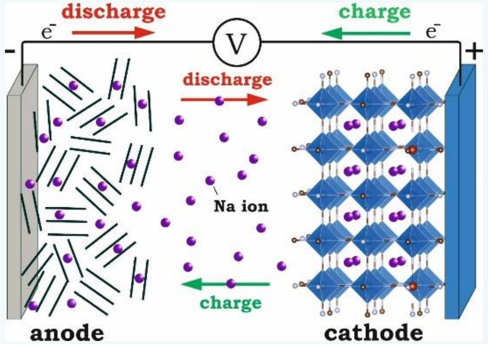

Principal scheme of SIB

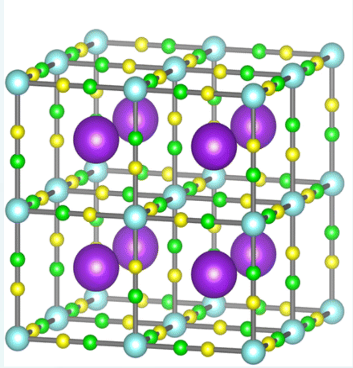

Structure of Prussian white

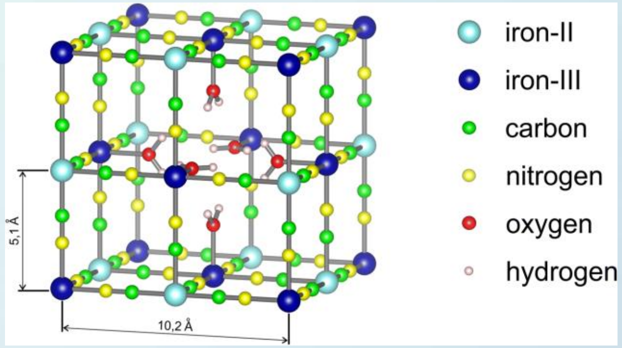

$Na_{2-x}Fe[Fe(CN)_6]_{1-y}\cdot\square_y\cdot mH_2O$, $\square$ - $Fe(CN)_6$ vacancies.

Compound contains water.

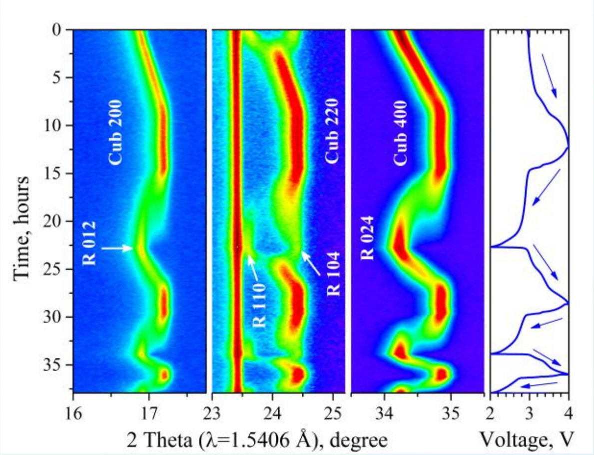

non-preheated electrode

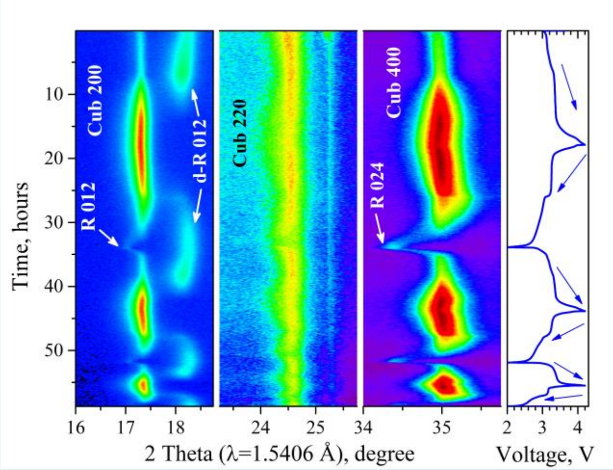

preheated at 200°C electrode

2D maps of diffraction pattens of the electrochemical cell with PW electrodes during charge - discharge cycles with different cycling rates.

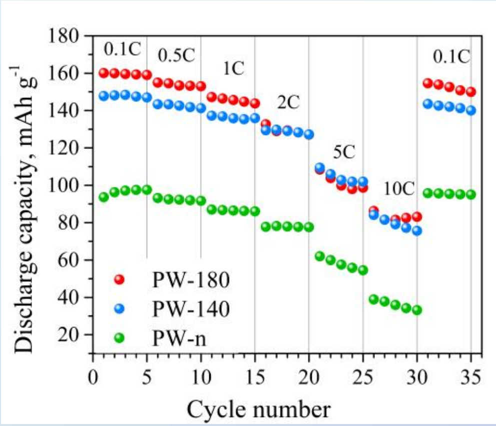

Capacity of the non-preheated (green), preheated at 140°C (blue) and 180°C (red) electrodes at different cycling rates.

Preheating the electrodes promotes the formation of dehydrated rhombohedral d-R phase, resulting in higher capacity compared to electrodes without preheating.

N.Yu.Samoylova et al., J. Alloys Compd., 983, 173849 (2024)

JOINT INSTITUTE FOR NUCLEAR RESEARCH

FLNP FRANK LABORATORY OF NEUTRON PHYSICS

Neutron scattering in condensed matter

Small Angle Scattering

Experimental facilities

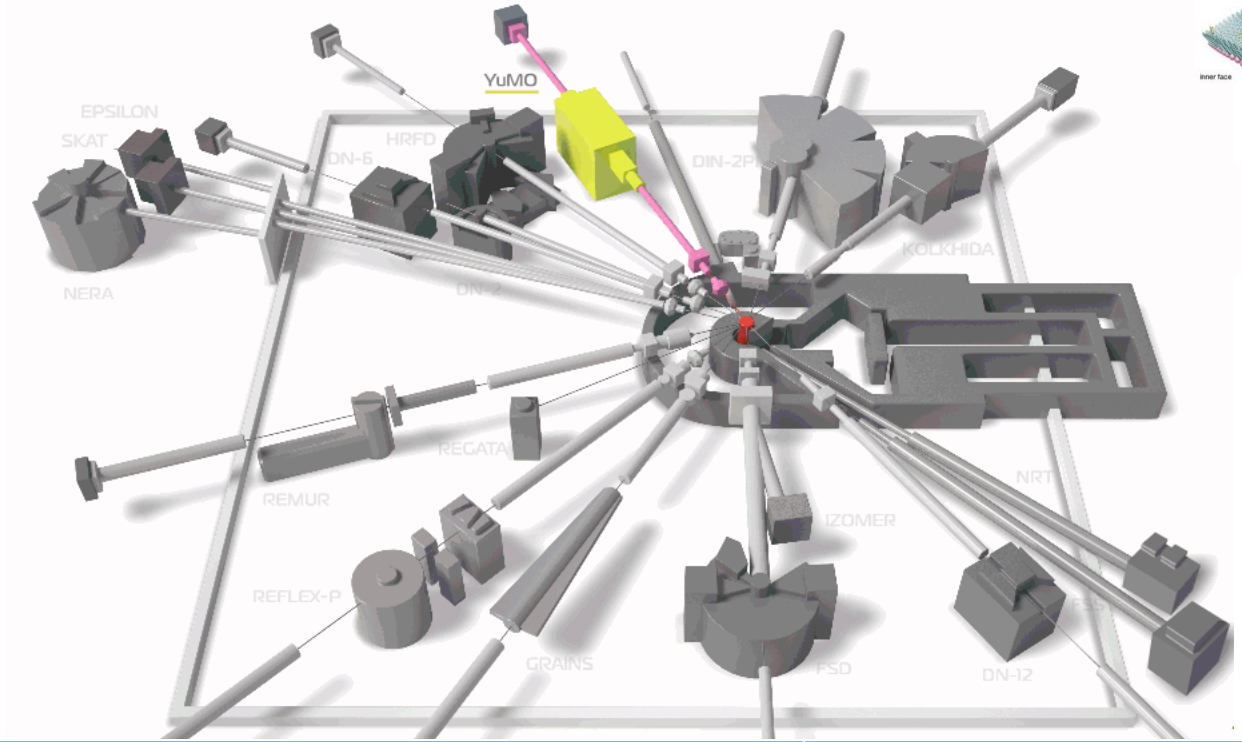

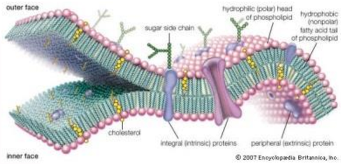

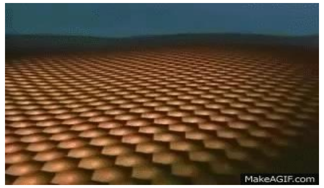

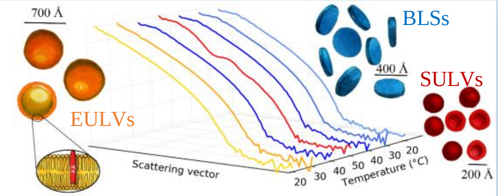

Small-angle scattering
YuMO

- **Structural organization** and **aggregation** of nanoparticles and **composite systems**
- Interactions of **nanoparticles** with **bio-macromolecules**

Applications	Basic parameters	Specific features
Determination of sizes, shapes, spatial correlations of particles, agglomerates, pores, as well as fractal dimension in nanomaterials, biological objects, polymers, colloidal solutions	Q-range: **7×10^{-3} - 0.5 Å^{-1}** Temperature range: 10-180°C	Characteristic particle size that can be identified: **1-500 nm** Minimum sample volume: **500 µl** Characteristic sample size is up to 1.4 cm in diameter

B I O H Y B R I D   N A N O C O M P L E X E S

based on phytogenerated Ag/AgCl NPs, biomimetic membranes and chitosan

AND THEIR POTENTIAL APPLICATION IN BIOMEDICINE

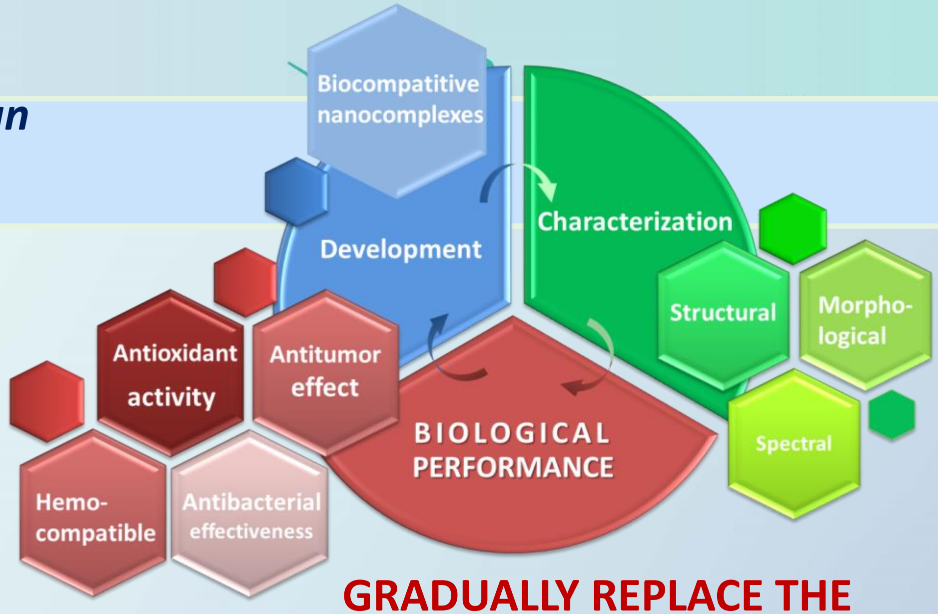

Formation of biohybrids

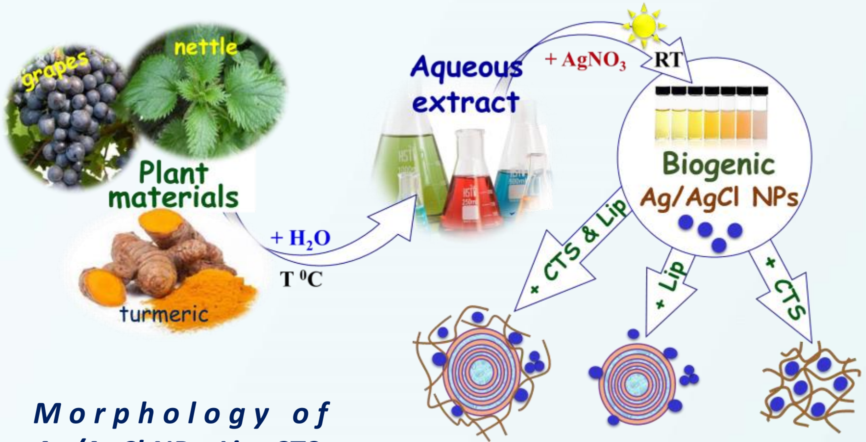

Structure of biohybrid components

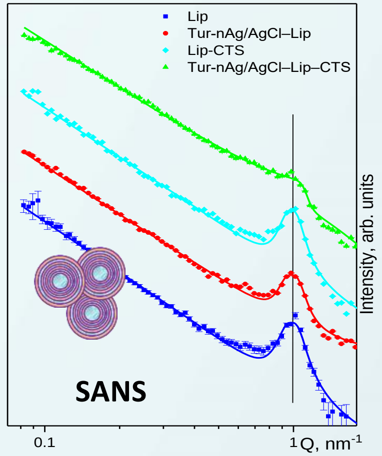

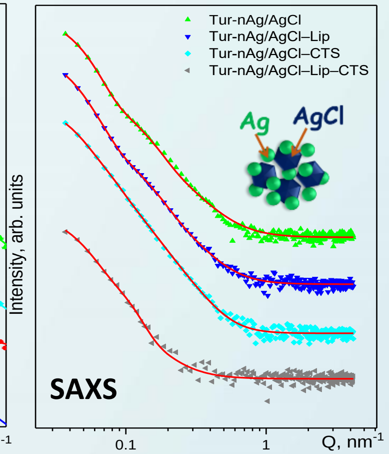

Morphology of Ag/AgCl NPs–Lip–CTS

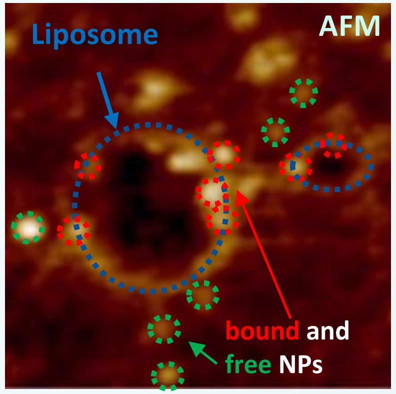

GRADUALLY REPLACE THE OLD-GENERATION DRUGS

that certainly have lost their "tooth" against the resistant microbes

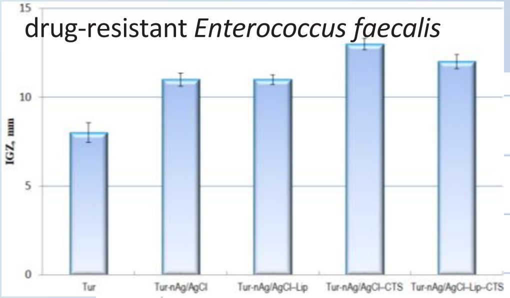

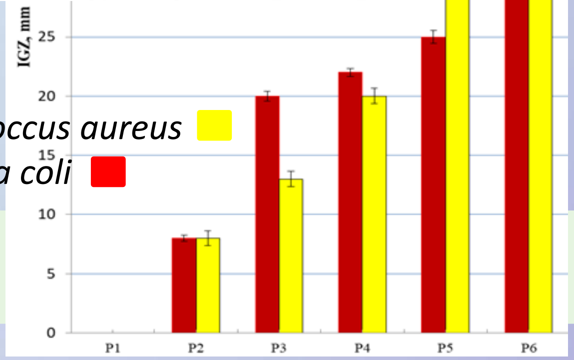

Staphylococcus aureus

Escherichia coli

ANTIPROLIFERATIVE ACTIVITY OF BIOHYBRID Ag/AgCl NPs–Lip–CTS

therapeutic index value of 1.30 for HT-29 cancer cells and 1.77 for HepG2 cancer cells

HT-29 cancer cells

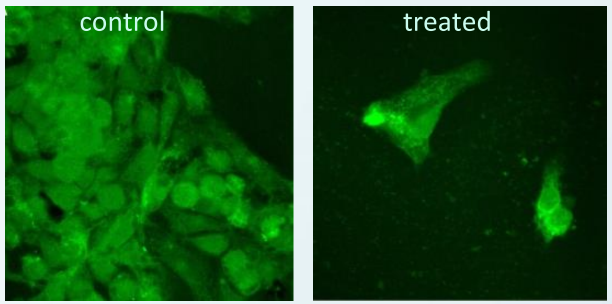

HepG2 cancer cells

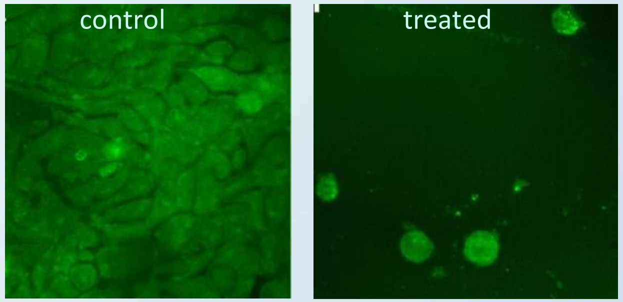

M.-E.Barbinta-Patrascu, Yu.Gorshkova; et al. Materials 14, 4726 (2021).

Yu. Gorshkova, M.-E.Barbinta-Patrascu; et al. Nanomaterials, 11, 1811 (2021).

FLNP JOINT INSTITUTE FOR NUCLEAR RESEARCH JINR
UNIVERSITATEA DIN BUCUREȘTI
UNIVERSITATEA POLITEHNICA DIN BUCUREȘTI
National Institute for Laser, Plasma and Radiation Physics
IFJ PAN
INSTITUTE OF MACROMOLECULAR CHEMISTRY

STRUCTURAL MODICIATIONS IN LIPID OBJECTS AT PRESENCE OF AMYLOID-BETA PEPTIDE

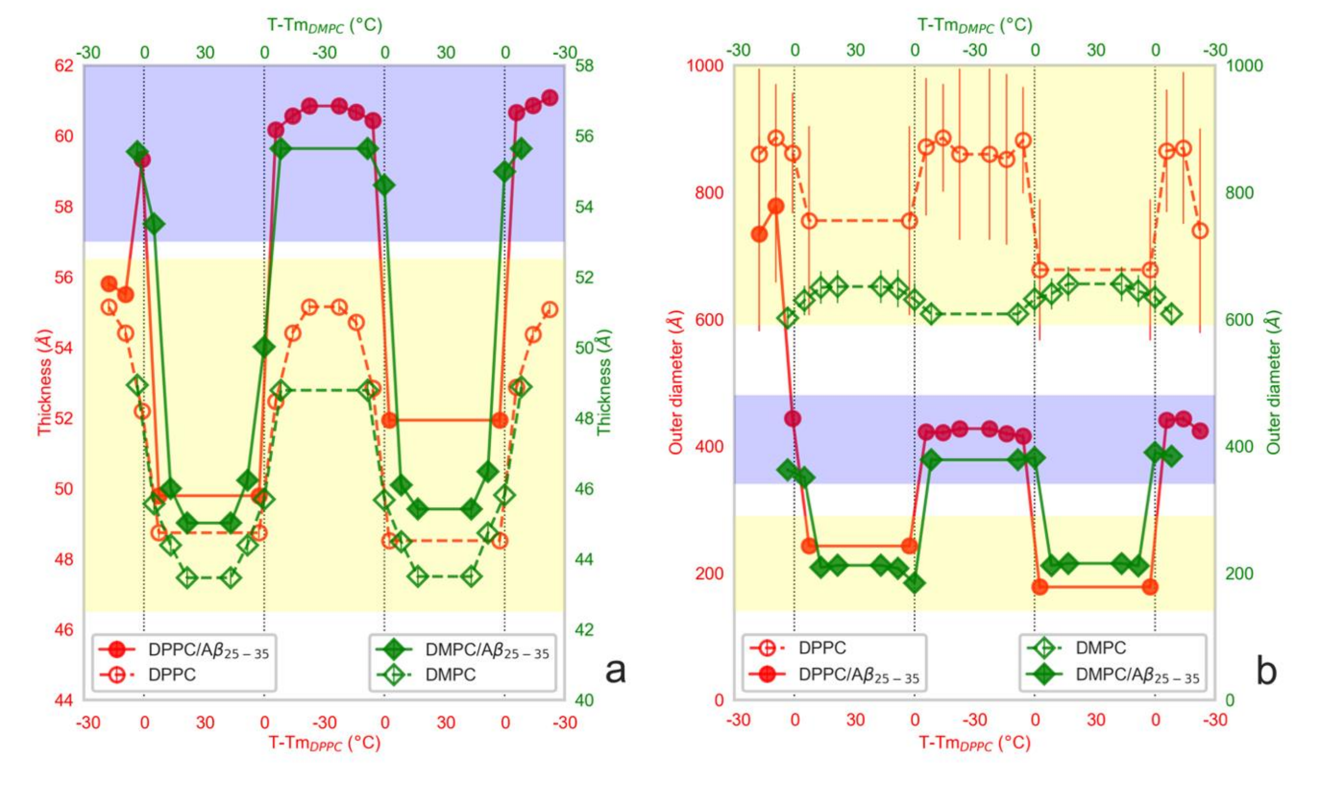

Thickness variation of the model membrane (a) and aggregate sizes (b) depending on temperature shift relatively to the main phase transition for DMPS ДМФХ (green rhombuses) and DPPC (red circles) with and without addition of amyloid-beta peptide.

O.I.Ivankov et al., Scientific Reports 11, 21990 (2021)

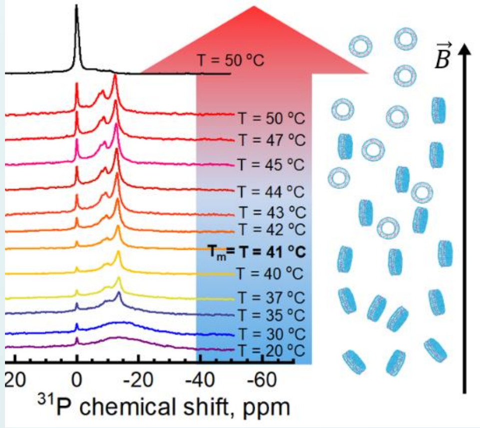

^{31}P NMR Spectra

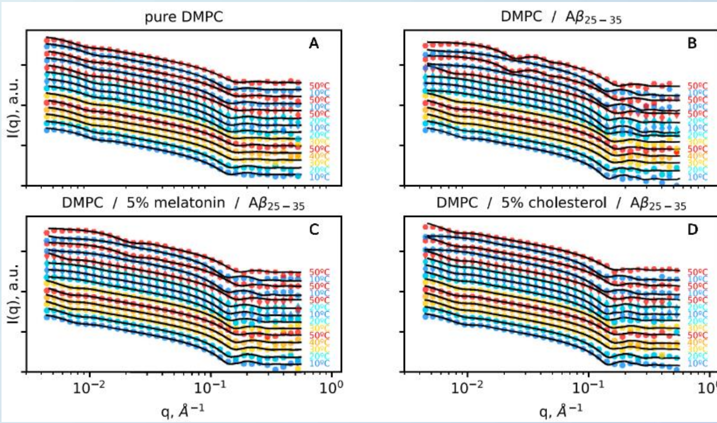

SANS curves

Saturated phospholipids + Aβ(25-35) peptides

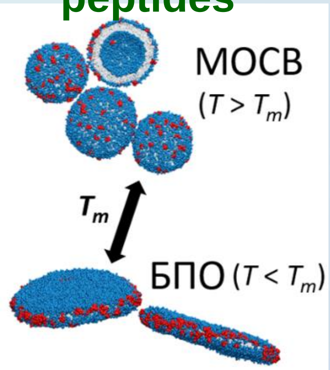

Aβ(25-35) peptides form predominantly unsaturated disordered structures

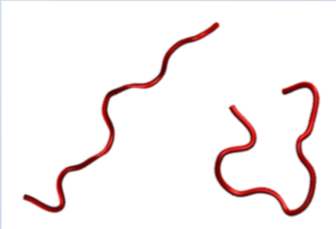

Random coils

β turns

S.A.Kurakin et al., Biochimica et Biophysica Acta – Biomembranes, 1866, 184237 (2024)
O.I.Ivankov et al., Scientific Reports 11, 21990 (2021)

Neutron scattering in condensed matter

Reflectometry

Experimental facilities

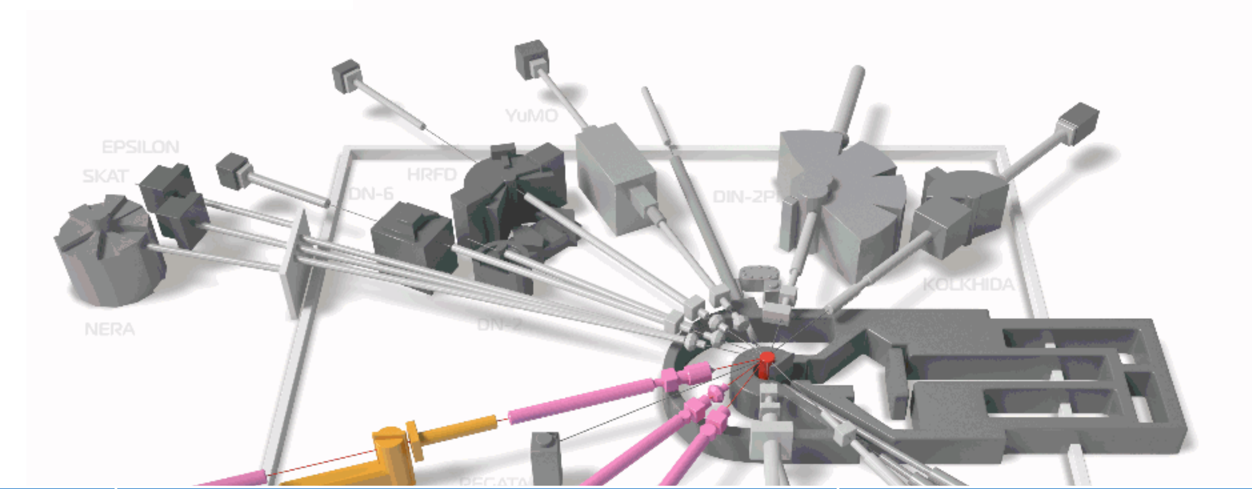

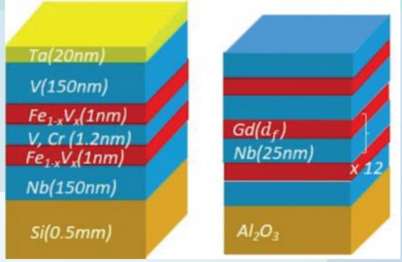

- **Thin films** and surfaces
- **Surface adsorption** of magnetic nanoparticles
- Superconducting and magnetic properties of the **complex layered heterostructures**

Reflectometry
GRAINS, REFLEX-P, REMUR

Spectrometer, Instrument	Applications	Basic parameters	Specific features
REMUR	Determination of parameters of magnetic and superconducting heterostructures, nonmetallic thin films	Q-range: 0.001 - 2 nm^{-1}, resolution $\Delta Q/Q \approx 1$ % Temperature range: 1.5 - 300 K Magnetic field on the sample: up to 1.5 T	Minimum surface area of the sample – 5x5 mm^2, thickness of layers accessible for research – **0.5-500 nm**, roughness – ~1 nm
REFLEX	Determination of structural parameters of thin-film nanostructures	Q-range: 0.01 - 1.3 nm^{-1}, resolution $\Delta Q/Q \approx 1 - 15$ % Temperature range: 1.5 - 300 K Magnetic field on the sample: up to 0.5 T	Minimum surface area of the sample – 20x20 mm^2, thickness of layers accessible for research – **2-500 nm**, roughness – ~3 nm
GRAINS	Determination of structural parameters of **interfaces with “soft” and liquid media**	Q-range: 0.05 - 1.0 nm^{-1}, resolution $\Delta Q/Q \approx 5$ %. Temperature range: 10 - 150°C	Minimum surface area of the sample – 5x5 cm, maximum interface thickness – **100 nm**, roughness – up to 5 nm (at a thickness of 100 nm)

A Study of Relationship between Magnetic and Superconducting Order Parameters at the Interfaces in Layered Helical Magnets Nanostructures

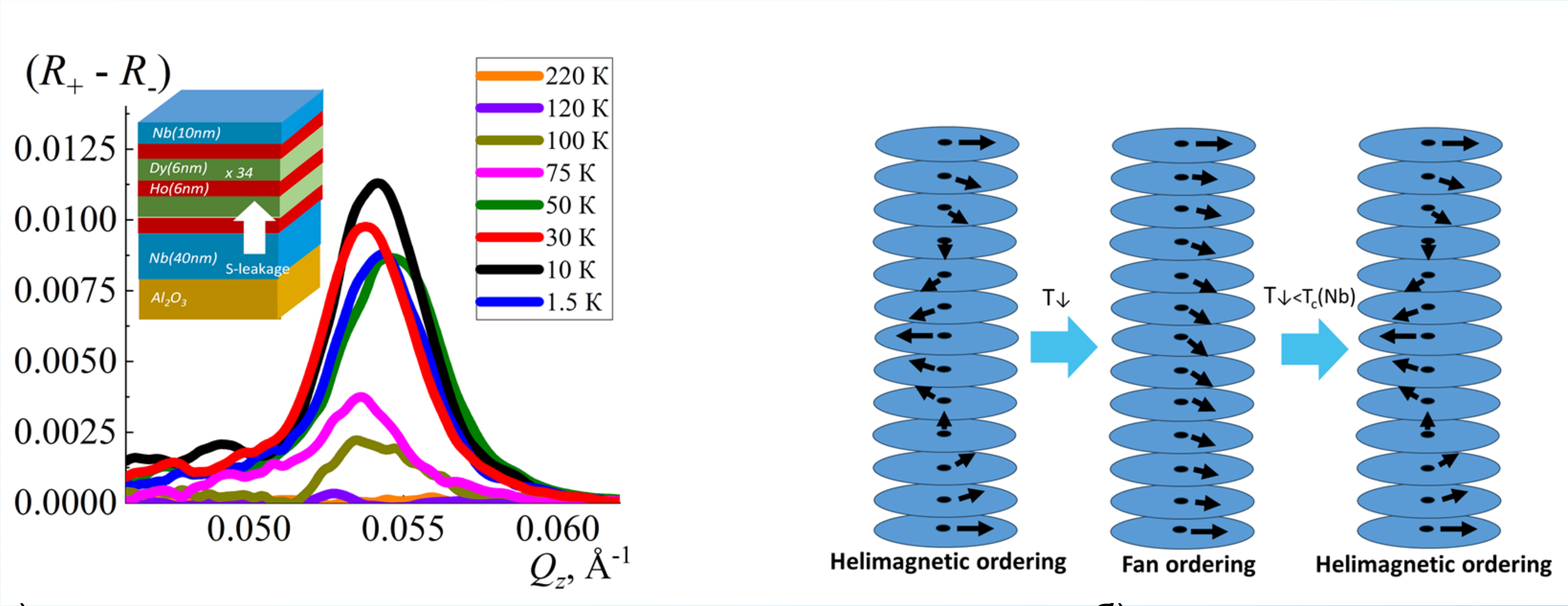

а) б)

(a) Difference of neutron reflection coefficients obtained at different temperatures in magnetic field of H = 1 кOe. (б) Modification of magnetic order of layered nanostructure on cooling: magnetic helicoidal arrangement is transformed to magnetic fan arrangement, below superconducting temperature the reverse transformation to helicoidal arrangement occurs.

V.D. Zhaketov, et al., Physics of the Solid State, 65, No. 7, 1076 – 1080 (2023)

Impact of cholesterol / melatonin on structure of model lipid membranes

Changes in cholesterol and melatonin concentrations affect **development of degenerative diseases**

Neutron reflectometry @ IBR-2

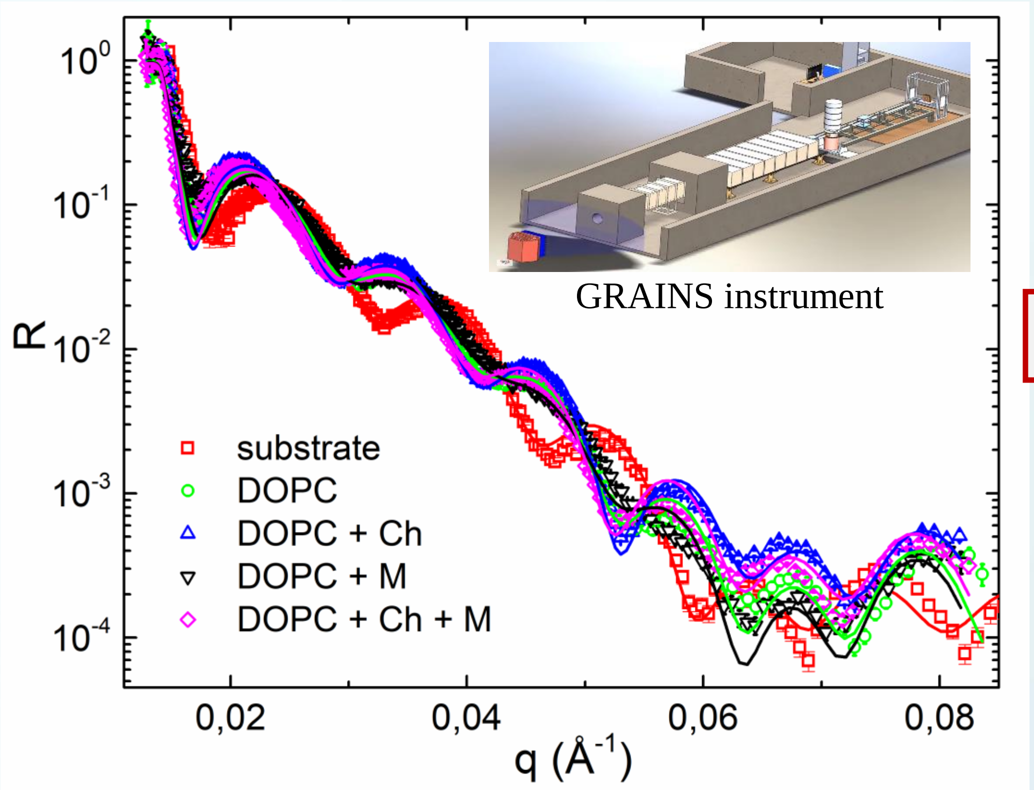

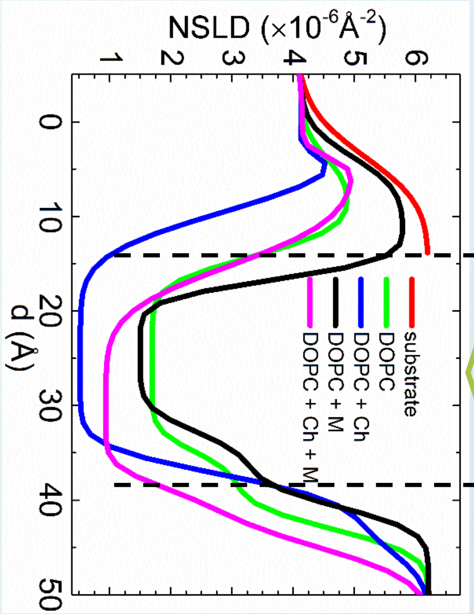

Molecular dynamics (FLNP, LRB)

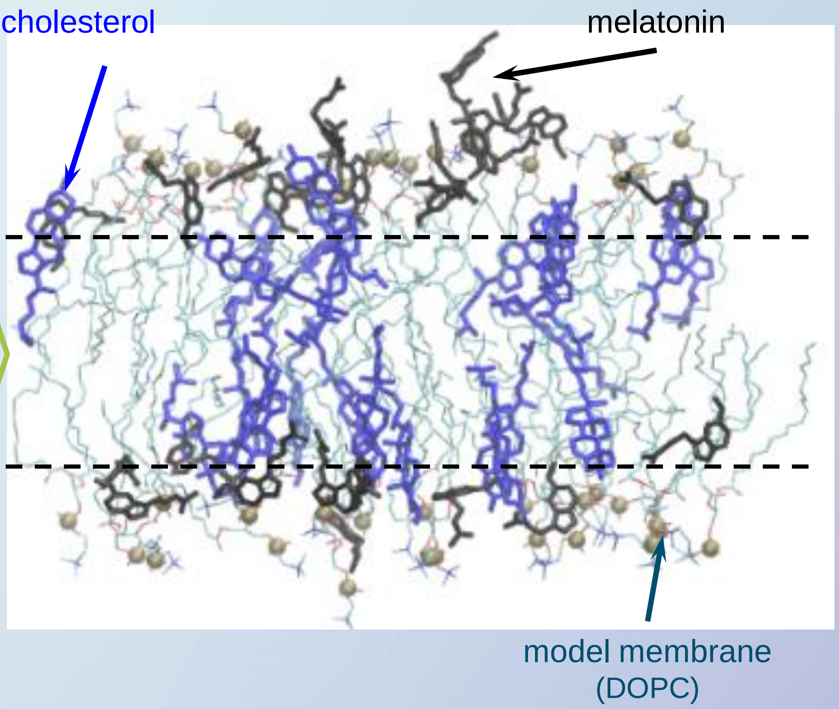

Cholesterol and melatonin found to **accumulate in different membrane regions**, affecting the entire structure of membrane (and its properties).

Hrubovčák P., Dushanov E., Kondela T., Tomchuk O., Kholmurodov K., Kučerka N., “Reflectometry and molecular dynamics study of the impact of cholesterol and melatonin on model lipid membranes” // **European Biophysics Journal**, 2021.

Neutron scattering in condensed matter physics

Inelastic Scattering

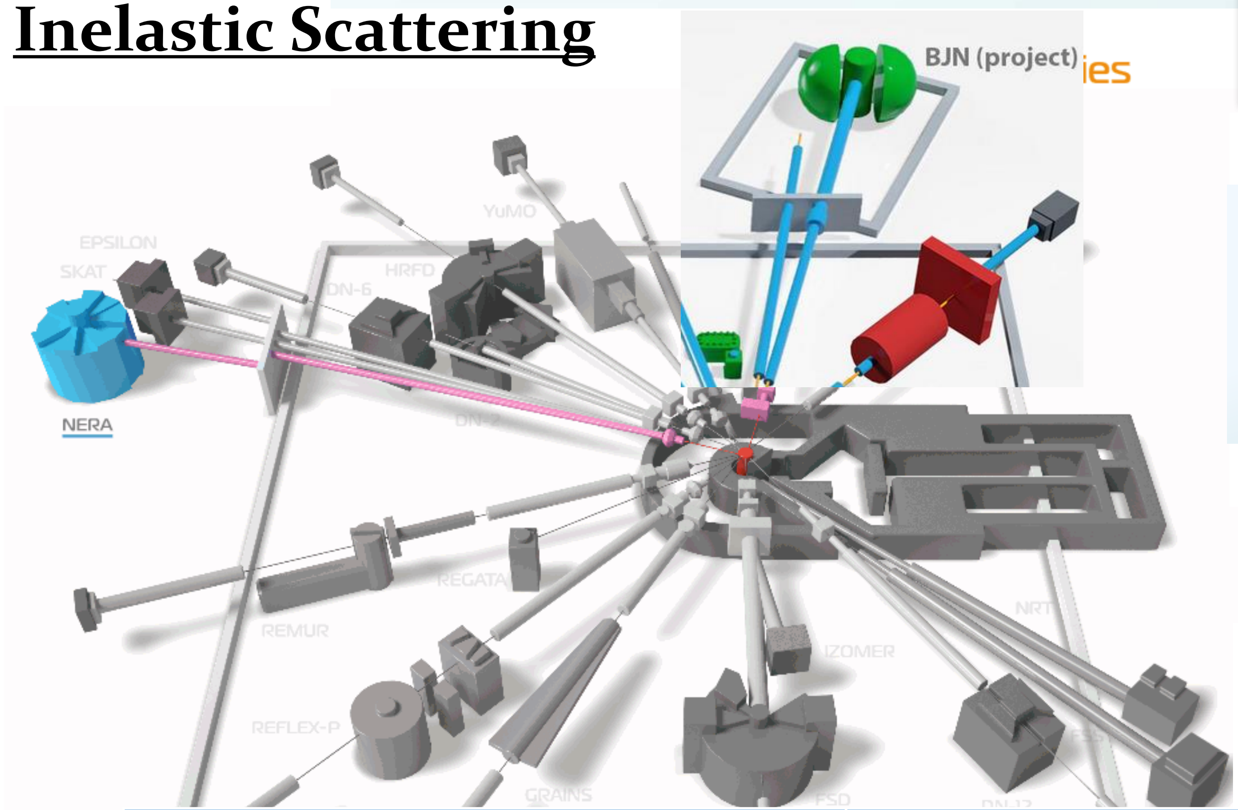

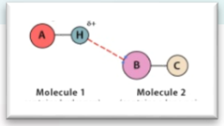

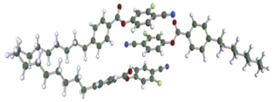

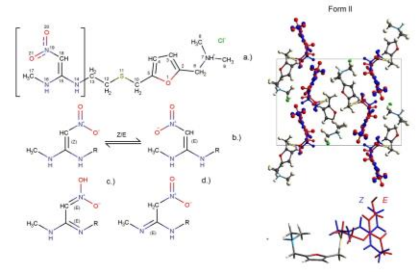

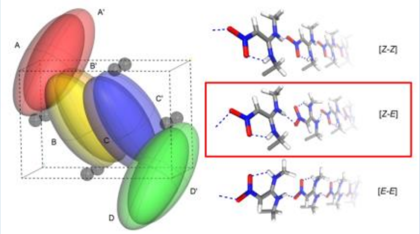

- Molecular structure and **dynamics**
- **Isomeric forms** of drugs
- **Drug delivery systems**

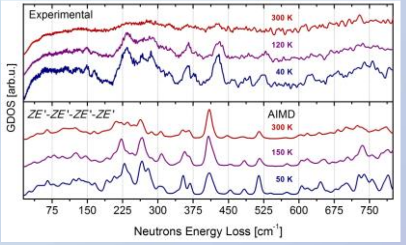

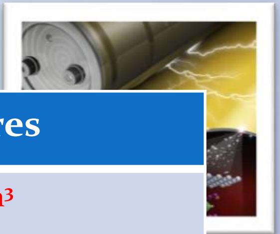

Applications	Basic parameters	Specific features
Investigation of atomic and molecular dynamics of hydrogen-containing compounds, including pharmacological substances, analysis of the effect of phase polymorphism	Energy transfer range: **1 - 160 meV** Resolution $\Delta E/E \approx$ 2- 4% Temperature range: 4 - 300 K	Sample volume is about **4-5 cm^3**

Example from NERA

Subject

Pharmacological drugs
used for neuropathic pain, epilepsy or other neuromuscular syndromes (ethosuximide - ETX)

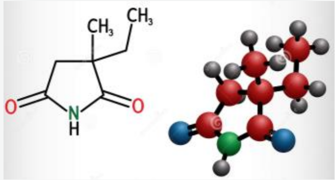

Method

Analysis of oscillation dynamics obtained from the density of states G(v) obtained from inelastic neutron scattering spectra (NERA Spectrometer, FLNP JINR, Dubna).

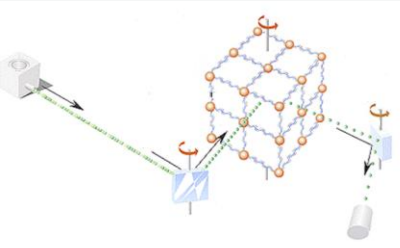

Target

The dynamic range available on the HEPA spectrometer in (Q,ω) neutron scattering space makes it possible to **characterize the vibrational dynamics of individual conformers, conformational changes and intermolecular motions.**

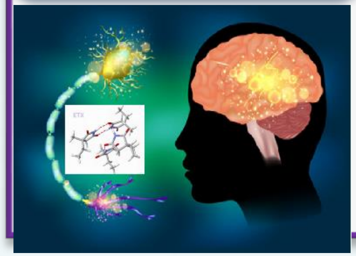

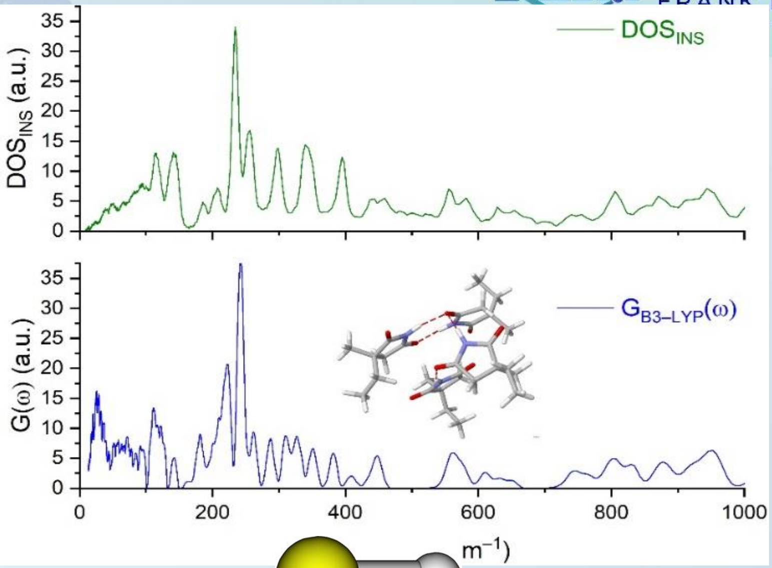

vibrational modes

ν – stretching,
β – bending in-plane,
γ – bending out-of-plane,
ρ – rocking, τ – twisting,
ω – wagging,
σ – scissoring,
χ – torsion

stretching
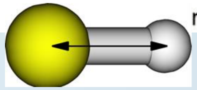
bending
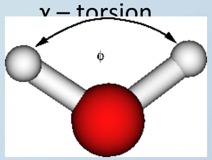
torsion
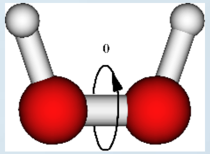
wagging
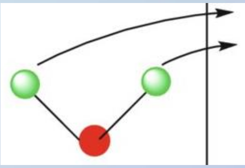

Calculated wavenumber (cm^{-1}) RS-ETX octamer/optimal conformation	G(ω)	Assignment
148	143	χCC + γCN
805	805	ωCH + γNH
886	880	γNH + νCC
939	943	νCC

N.Osiecka-Drewniak, et al., Spectrochim. Acta Part A: Molecular and Biomolecular Spectroscopy, Vol. 279, 2022, 121468, https://doi.org/10.1016/j.saa.2022.121468

Neutron radiography and tomography station (NRT)

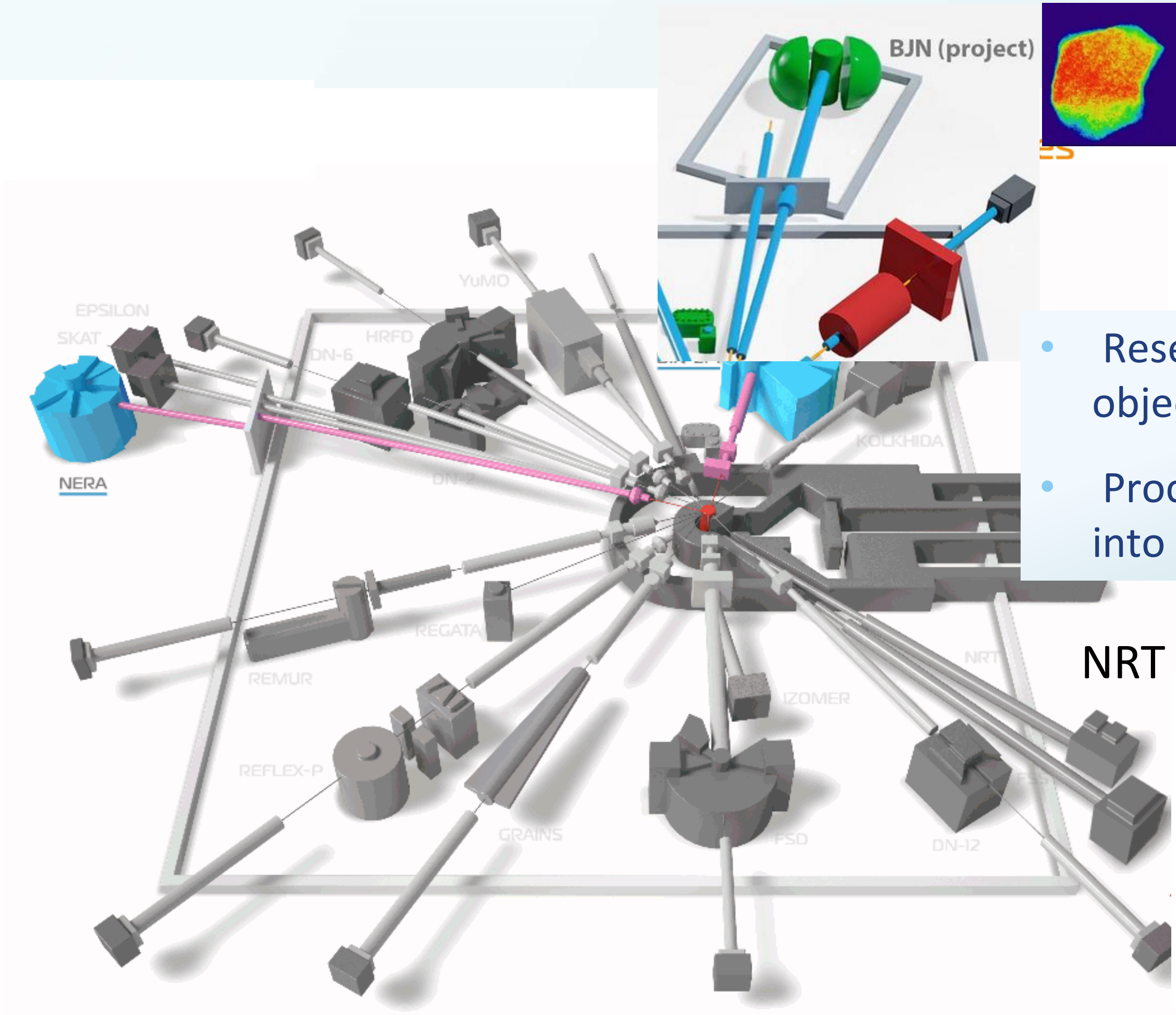

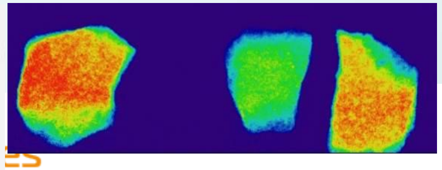

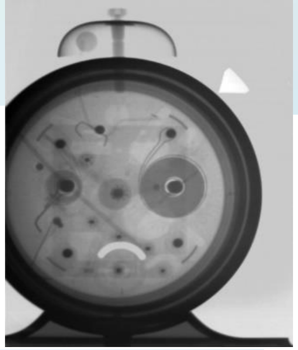

- Research of internal structure of objects
- Processes of water penetration into materials

NRT

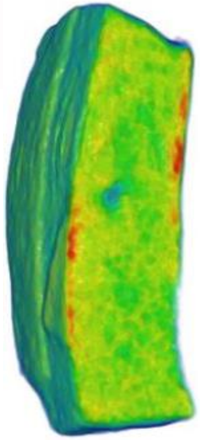

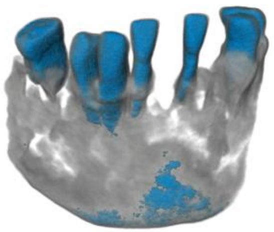

THE SYSTEMATIC STRUCTURAL STUDIES OF SOME BYZANTINE CERAMIC FRAGMENTS FROM DOBRUDJA REGION OF ROMANIA

JOINT INSTITUTE

FLNP FRANK LABORATORY OF NEUTRON PHYSICS

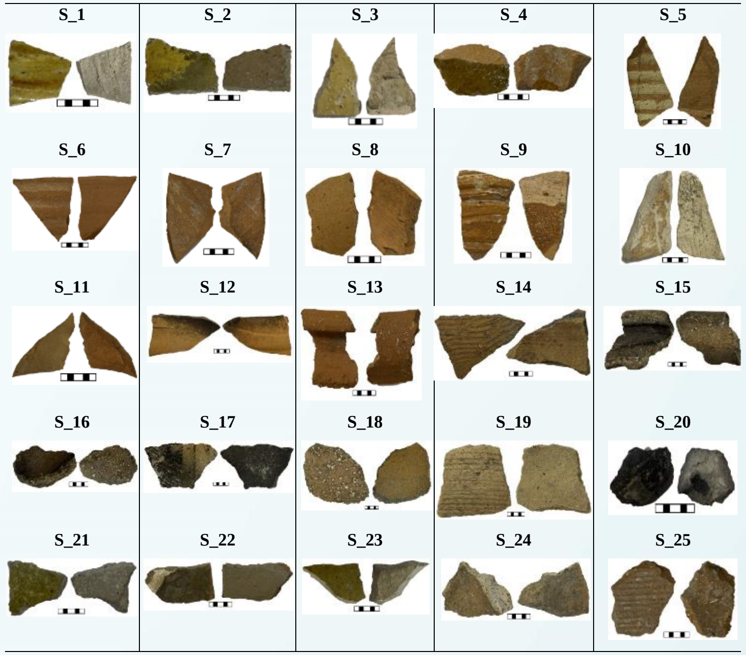

Neutron tomography, neutron diffraction, Raman spectroscopy

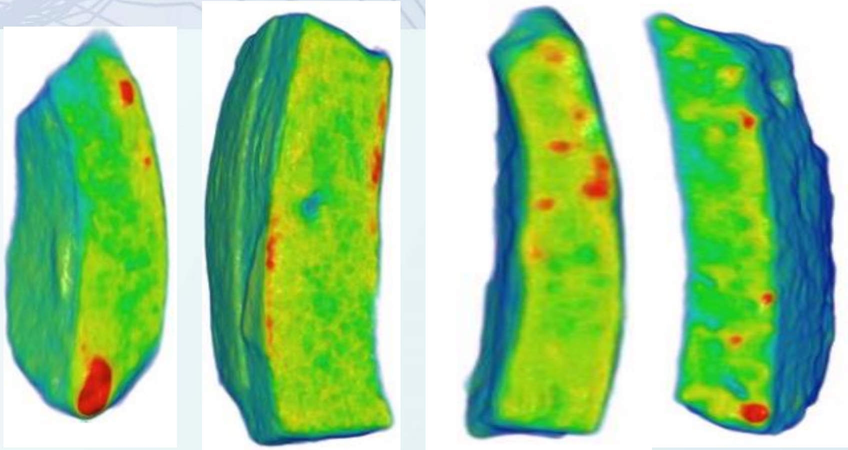

3D models – neutron tomography

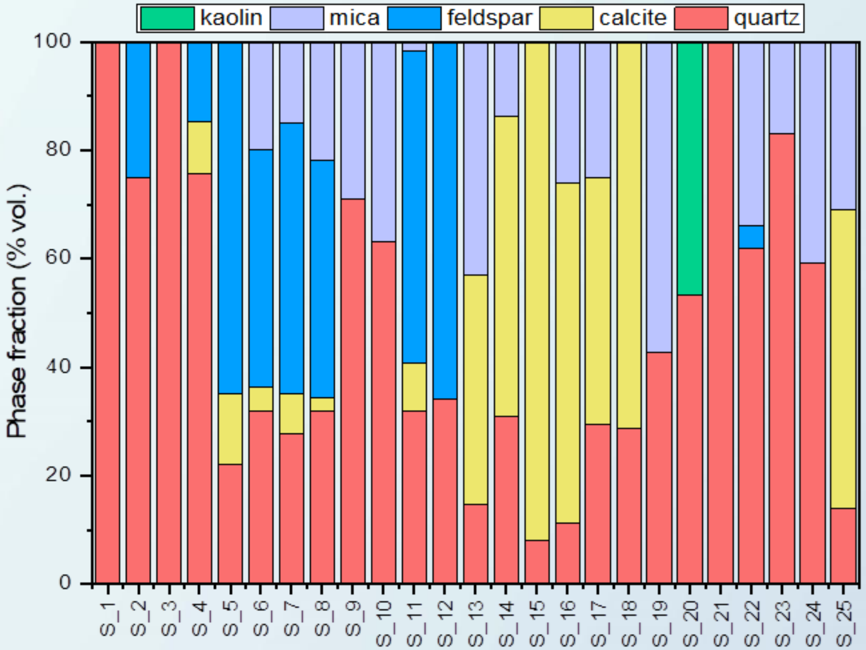

Phase analysis – neutron diffraction

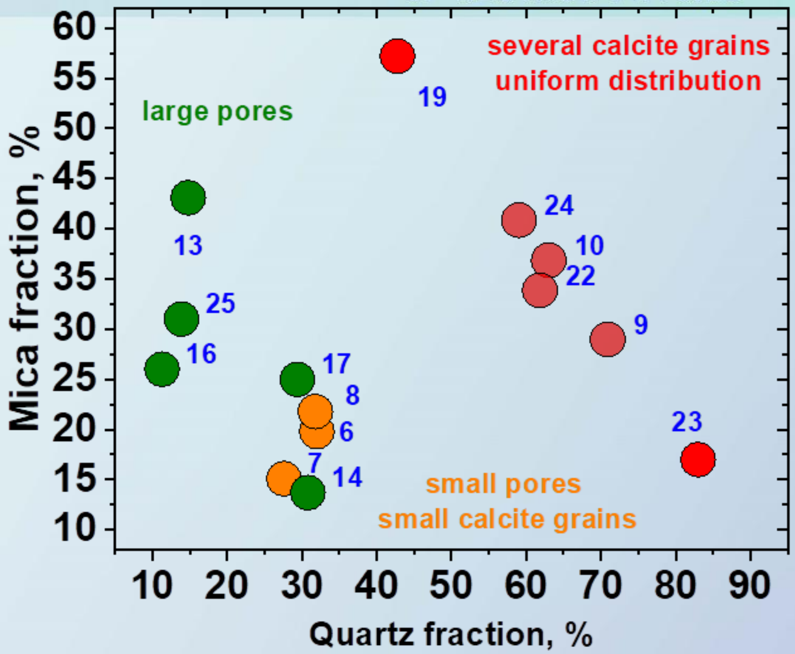

Grouping by structural attributes

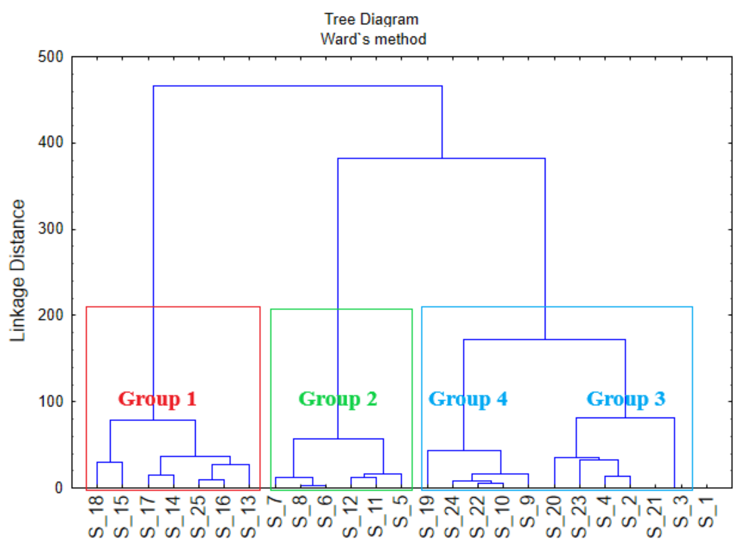

Zhomartova, A. Z., Abdurakhimov, B. A., Talmațchi, C. and et al (2024). Archaeometry, 1–16. https://doi.org/10.1111/arcm.12947

Nuclear analytical method

Neutron Activation Analysis

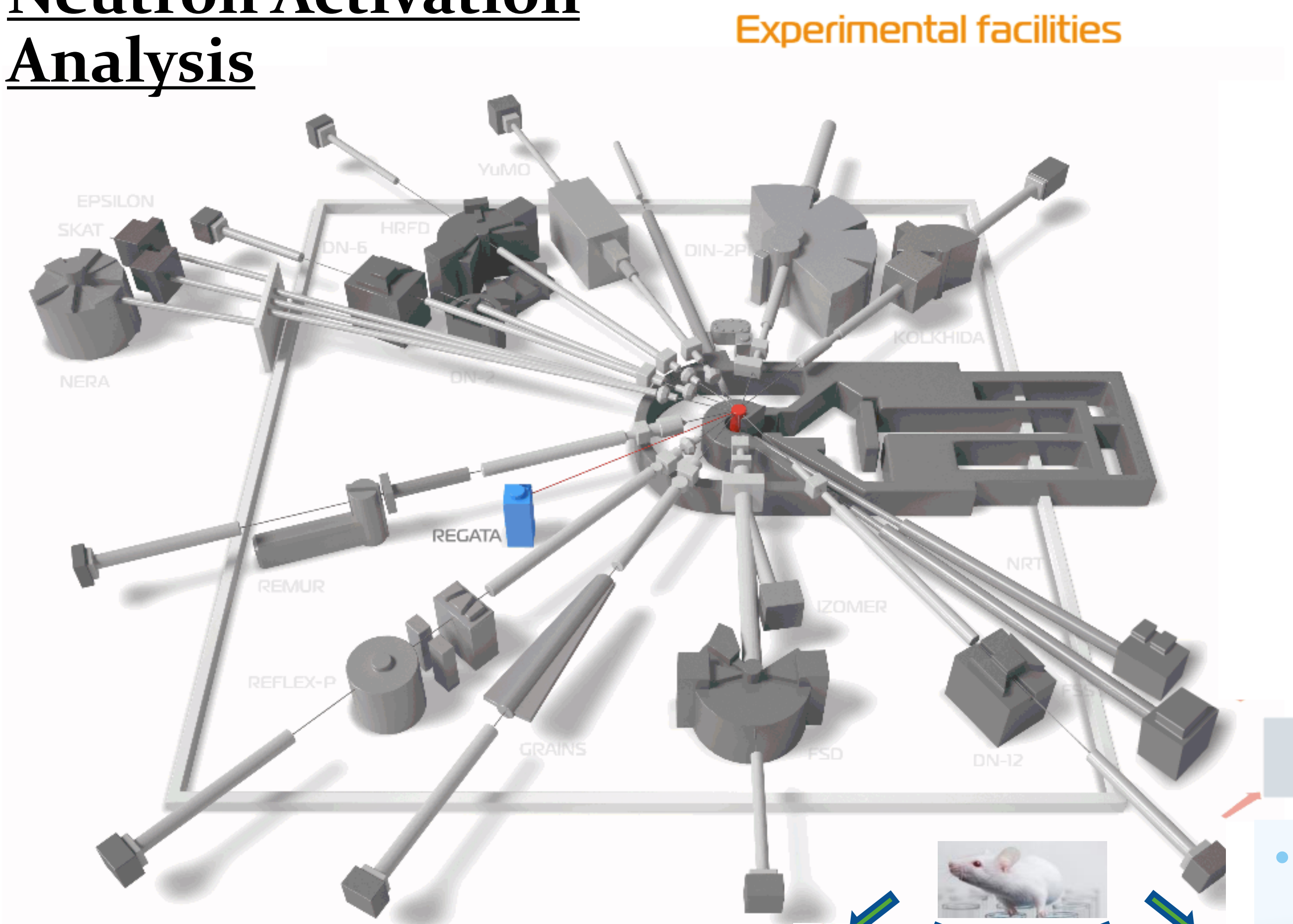

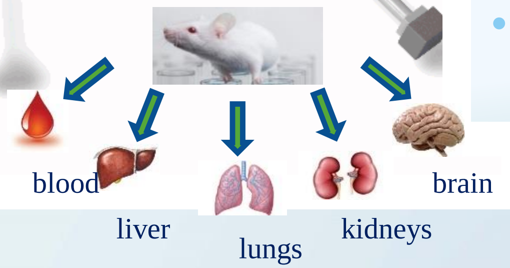

UNECE
United Nations
United Nations Economic Commission for Europe

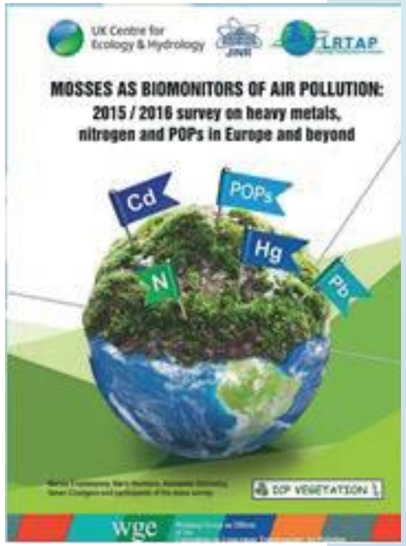

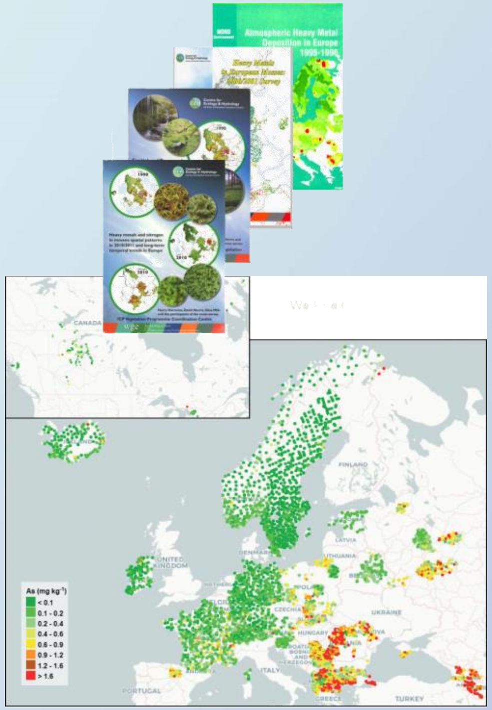

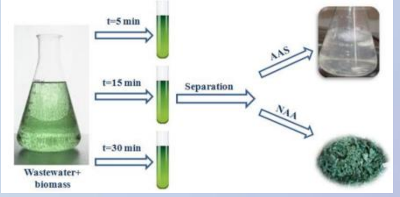

Neutron Activation Analysis
REGATA

- **Elemental composition analysis** of air, water, and soil or objects of cultural heritage

Scientific highlights

Development of the biological approach for rare earth elements recovery from wastewater

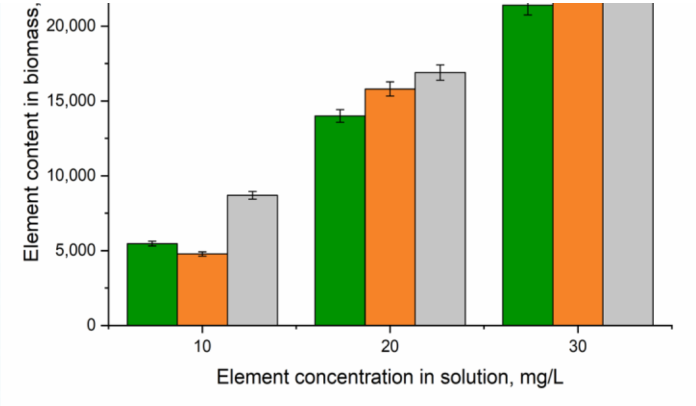

Uptake of Er, Ho, and Gd by *spirulina* biomass cultivated in a medium supplemented with REEs.

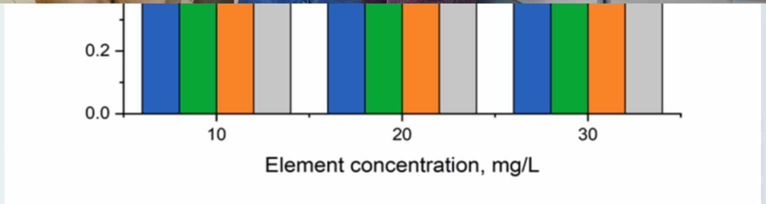

Effects of rare earth elements on spirulina productivity

I. Zinicovscaia et al. Microorganisms, 12, 122. (2024)

FLNP offers a large suite of equipment for comprehensive study of samples by complementary techniques

It includes:

- Xeuss 3.0 X-ray scattering station;
- X-ray Diffractometer EMPYREAN (PANalytical);
- Coherent Anti-Stokes Raman Spectrometer
- Raman spectrometers;
- IR and UV spectrometers;
- RFA;
- ICP-MS
- Chromatography System NGC Quest™ 10 Plus
- AFMs
- …etc.

https://flnp.jinr.int/images/box-slider/Laboratory_Equipment_DNICM_FLNP_JINR_2021.pdf

Main activities in the field of nuclear physics with neutrons:

1. **Investigations of the neutron induced nuclear reactions:**
   - fundamental symmetries;
   - highly excited states of the nuclei;
   - nuclear fission;
   - nuclear data.

2. **Investigations of the fundamental properties of the neutron, ultra-cold neutrons:**
   - tests of quantum mechanics;
   - search for new type of interactions;
   - neutron lifetime measurement.

3. **Applied and methodical research:**
   - neutron activation analysis and others nuclear technics for isotope analysis;
   - neutron in space;
   - Ion beam analysis:
   - IREN developing.

Source of resonance neutrons IREN based at lineal electron accelerator

https://flnp.jinr.int/en-us/main/facilities/iren

The linear electron accelerator LUE-200 used as a driver for the intense resonance neutron source IREN. The accelerator is positioned vertically. It consists of a pulsed electron gun, an accelerating system, microwave power sources based on 10-cm klystrons with modulators, a focusing-beam transport system, a diagnostics system with a broadband magnetic spectrometer and a vacuum system.

Peak current (A)	3
Repetition rate (Hz)	50
Electron pulse duration (ns)	100
Electron energy (MeV)	110
Beam power (kW)	1.5
Multiplication	1
Neutron intensity (n/s)	~$3x10^{11}$

1200 hours/year

D-T generator for tagged neutron technique (TANGRA Project)

https://flnp.jinr.int/en-us/main/facilities/tangra-project-en

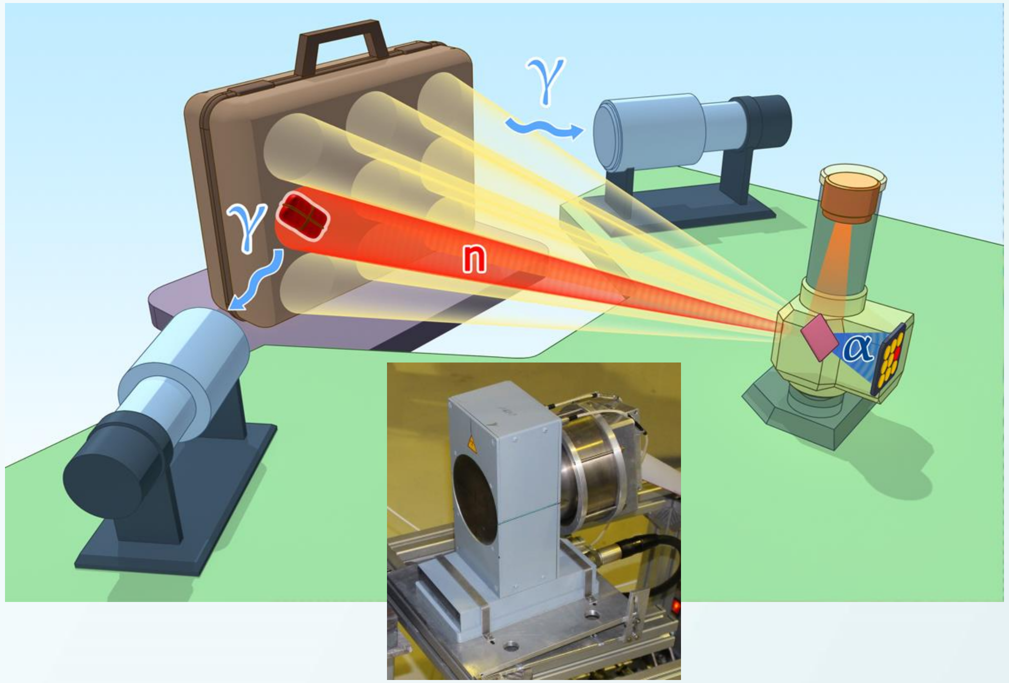

yield up to 10^8 c^{-1}
Set of NaI(Tl) detectors
Set of BGO detectors
Set of LaBr detectors
Set of detectors based on different plastics
HPGe detector

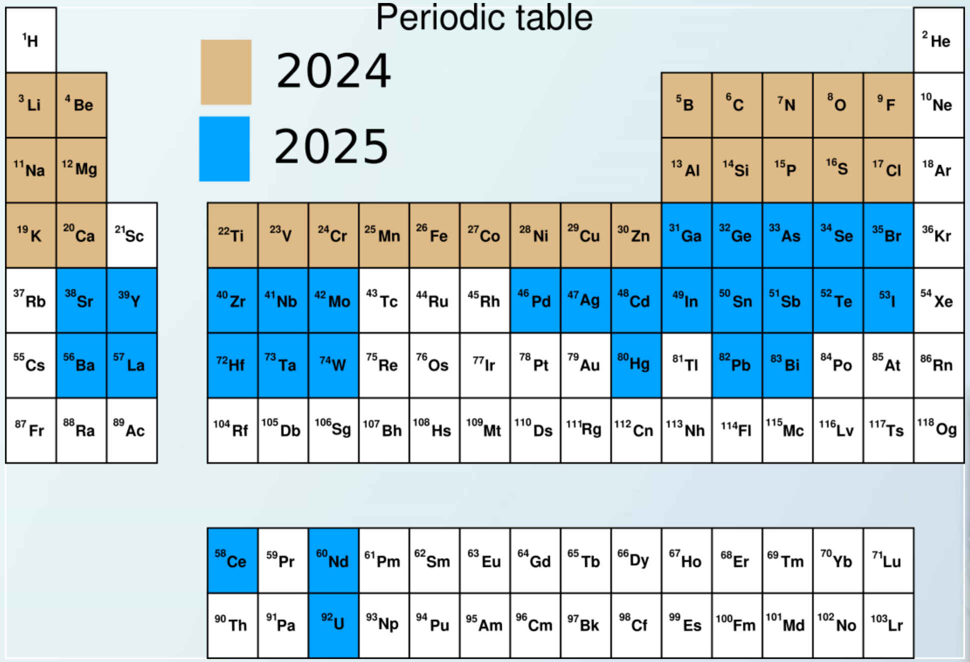

In 2024 γ-ray emission cross sections for light elements was measured: B, C, N, O, F, Na, Mg, Al, Si, P, S, Cl, K, Ca, Ti, V, Cr, Mn, Fe, Co, Ni, Cu, Zn, Sn.

Gamma-spectra and angular distributions of gamma ray have been measured in inelastic neutron scattering reactions for 20 nuclei.

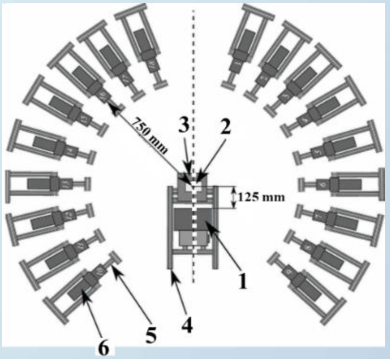

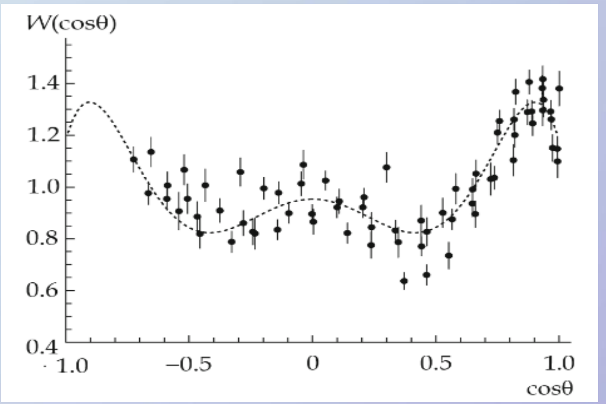

EG-5 https://flnp.jinr.int/en-us/main/facilities/eg-5

Electrostatic Van de Graaff accelerator, was built in 1965.

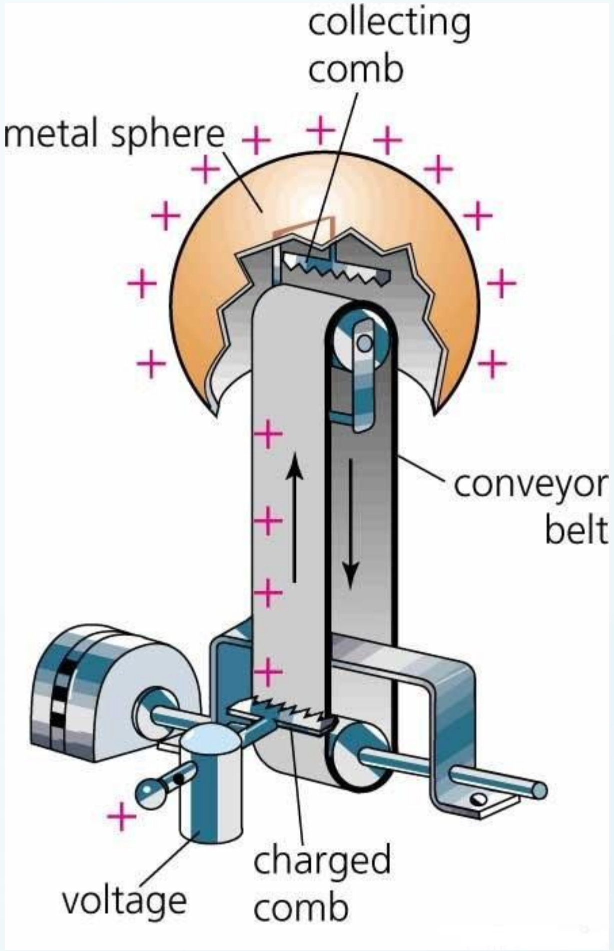

The installation remains in demand today.

The characteristics of EG-5 Accelerator:	
Energy region	0.9 – 3.5 MeV
Beam intensity for H+	30 μA
Beam intensity for He+	10 μA
Energy spread	< 500 eV
Number of beam lines	6

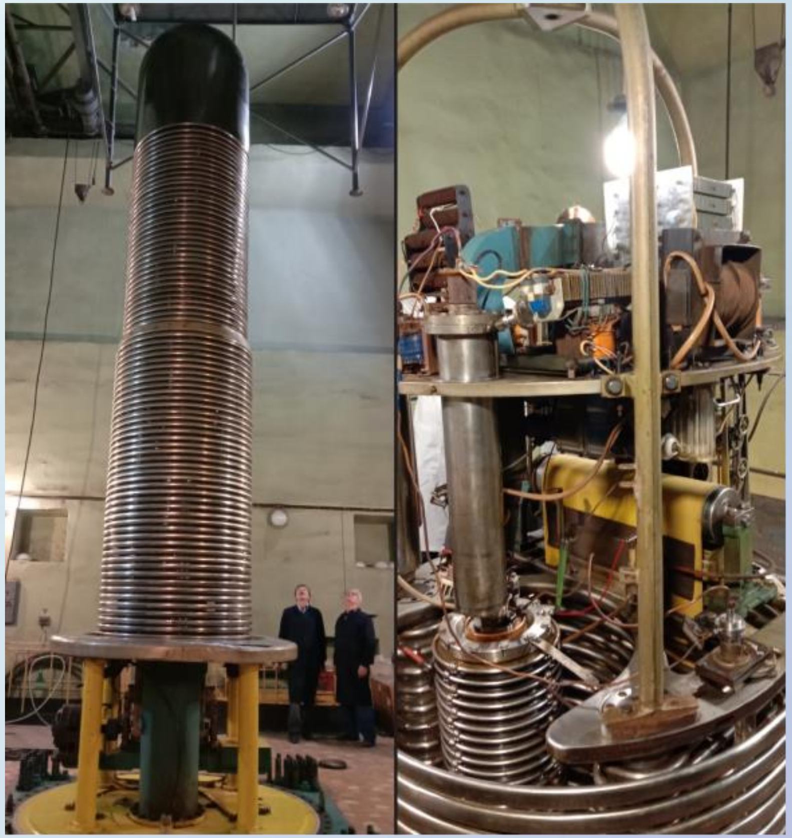

600 hours/year

Plan of modernization 2023-2026:

Before modernization	After modernization
Terminal voltage - 2,5 MV Beam current – 100nA Ion Energy – 2,5 MeV	Terminal voltage - **4,1 MV** Beam current – **50-100mkA** Ion Energy – **4,1 MeV**

Development of neutron instruments elements :

1. **Neutron detectors:**
   - gaseous and scintillator neutron detectors;
   - development of the technology of thin film B_4C coverage;
   - detector electronics.

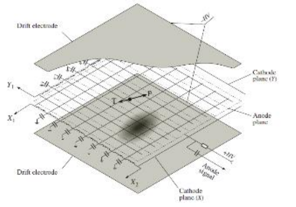

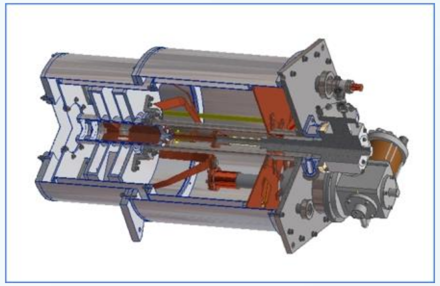

2. **Tools for instrument development and optimization:**
   - Simulation of instruments;
   - sample environment systems
   - Software.

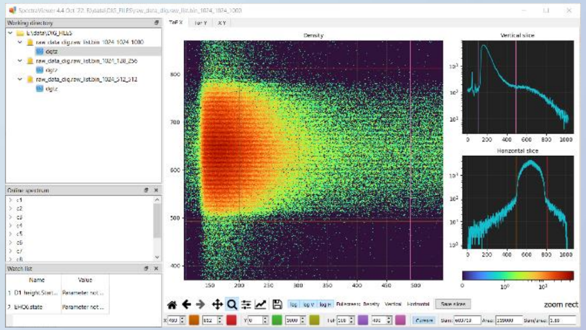

3. **Developing of cold moderators:**
   - developing of exist moderators' cryogenic system ;
   - developing of methane-based moderator.

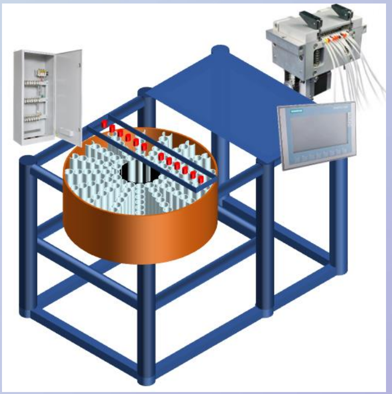

New back scattering detector

New large aperture ZnS scintillator detector system covering scattering angles range 2θ= 133-175°, installed at the HRFD diffractometer.

Ω, sr2

The surface of scintillator S > 10 m^2

The approximate length of fibers L=36000 m

Photomultipliers : 216

Experimental site for neutron detector production

Spattering machine for B_4C coverage

Ferry Vatt company, Kazan, Russia

Max. coverage square 400x1200 mm²

Modern equipment and engineer systems

Thank you for attention
and
we invite you to joint research